EMBEDDED AND RF POWERED IMPLANTABLE MEDICAL DEVICE FOR GASTRIC ELECTRICAL STIMULATION (GES)

by

GURU MOORTHY RAVI

Presented to the Faculty of the Graduate School of

The University of Texas at Arlington in Partial Fulfillment

of the Requirements

for the Degree of

MASTER OF SCIENCE IN ELECTRICAL ENGINEERING

THE UNIVERSITY OF TEXAS AT ARLINGTON

May 2013

ACKNOWLEDGEMENTS

I am grateful to Dr. Jung-Chih Chiao, my advisor and mentor, for his continuous support and belief in my abilities, which motivated me to stretch my limits and achieve this milestone in my research career. His knowledge, commitment and wisdom have provided me the opportunity to work on a multitude of projects. I deeply appreciate his suggestions, and guidance throughout this work. I am also thankful to him for providing financial assistance during my graduate study.

I am thankful to Dr. W. Alan Davis and Dr. William E Dillon for taking interest in my research and accepted to serve as members of my thesis dissertation committee.

I would like to give special thanks to Dr. Smitha M N Rao for introducing me to this amazing iMEMS group. My class project in Advanced MEMS course, which is taught by her, is one of the great motivations towards this thesis. Also, I would like to thank her for shaping up my presentation skills.

I would like to thank my colleagues Dr. Uday Shankar Tata, Dr. Young-Sik Seo, Philip McCorkle, Cuong M Nguyen, Nguyen Quoc Minh and Zach Hughes for their help with the experiments. I have really enjoyed being an iMEMS member. I would like to thank all the past and current members of iMEMS for their valuable suggestions.

I would like to express my deep gratitude to my father Mr. Ravi and my mother Mrs. Girija for their love and blessings. I would like to thank my brother Jagan and my whole family for their encouragement and support.

April 09, 2013

ABSTRACT

EMBEDDED AND RF POWERED IMPLANTABLE MEDICAL DEVICE FOR GASTRIC ELECTRICAL STIMULATION (GES)

Guru Moorthy Ravi, M.S

The University of Texas at Arlington, 2013

Supervising Professor: Jung-Chih Chiao

Gastric electrical stimulation (GES) has attracted significant attention in the treatment for Gastroparesis-a common disorder caused in patients suffering from diabetes, cancer and Parkinson's disease. Symptoms include vomiting, nausea, abdominal bloating etc. due to loss of motility in the stomach muscles. GES uses electrical pulses on the stomach tissues to help regain normal motility and reduce the symptoms. Conventional gastric stimulator needs a long surgery to be implanted and it is a big pacemaker like device that runs by a non-rechargeable battery. It has to be replaced once the battery gets exhausted every 5 to 6 years. Hence another round of surgery is done when these devices are needed to be replaced and re-implanted. This takes a heavy toll on patients both physically and financially. In many cases, insurance does not cover the cost of surgery and post-operative care. In this work, a battery-less implantable miniaturized wireless gastric stimulators for long term GES has been developed. Wireless telemetry for the devices is based on inductive coupling at a carrier frequency of 1.3 MHz from an external transmitter which also delivers power. The devices have been tested on a bench top experimental setup by acquiring Electrogastrogram (EGG) signals from the device which are recorded using a Data Acquisition (DAQ) system. The wireless power

transfer to the implant device has been demonstrated by testing different transmitter and receiver antenna configurations. Finally, an additional feature of reconfiguring the settings of the device is accomplished by a novel technique of using the carrier signal frequency. These results were well all within the requirements of the system.

TABLE OF CONTENTS

LIST OF ILLUSTRATIONS

Figure Page

LIST OF TABLES

Table Page

CHAPTER 1

INTRODUCTION

1.1 Motivation

In recent years people suffering from Gastroparesis have become increasingly large in number. In North America alone close to 1 million people suffer from this disease. Also, this is a widespread disease all over the world. The disease is treated by both drug based methods and also using implant methods. Many advances in medicinal cures and gastric electrical stimulation techniques have been tried and exploited for the treatment of the syndrome, but none of them were efficacious to eradicate this endemic completely. This work is focused on improvising implant based techniques. The currently available implant method uses a non-rechargeable stimulator called Enterra Therapy (from Medtronic Inc., shown in figure 2.3) has shown very promising results. In the past two decades, advances in wireless technologies not only revolutionized communication methods, but also used in varied fields including household applications, safety, security, education domains, and medical industry and so on. The reliability and cost effectiveness was always the major concern when it was about wireless technology associated with medical instruments.

Recently wireless technologies have transformed the scenario and attracted huge interest from healthcare industry. Many researchers and technologists have realized that the standard that can be accomplished by using wireless solutions cannot be realized by any other methodologies. The wireless method offers different solutions for therapy, diagnosis and curing. Since wires are often too large, insecure, uncomfortable or even not possible to be employed in some circumstances. In case of battery operated

devices the weight and volume of the device is very high, and it limits the implantation in certain medical conditions. Furthermore, the possibility of infection due to exposure of wires with the tissues raises a lot of issues in treating the patient. Conversely, the wireless technology provides a platform for the new level of progression to both medical device manufacturers and medical society by overcoming all these existing problems. Considering all these, designing a wireless medical device and delivering a less painful solution to treat gastroparesis is the main motive behind this project.

1.2 Objective

This thesis demonstrates the design and development of the miniaturized and wireless gastric stimulator and the relevant experimental results. The device prototype is tested with several bench top experiments and the device performance is monitored for different configurations.

The main objectives behind the development of miniaturized gastric stimulator are:

- To demonstrate a new way of delivering electric pulses to the stomach muscles for treating gastroparesis.
- To design wireless gastric stimulator using minimal passive and active components that is very small in contrast to existing devices.
- To design appropriate receive antenna and test it extensively for different transmitter configurations in order to be operated by wireless power externally. So that future surgeries to replace batteries will be prevented.
- To demonstrate the reconfiguration of stimulator setting without using any wireless communication IC. A new method of changing the settings based on transmitter frequency information is demonstrated in this work.

1.3 Proposed Design and Application

Implantable devices are very widely used in the medical industry for treating patients with different conditions. To name a few, pacemakers are used in treating people with heart diseases, neuro-stimulators in treating Parkinson's disease, cochlear implants and many more. Similarly, gastro-stimulators are widely used in recent times in treating gastroparesis, and it has made significant progress in many cases.

The most widely used currently available device for treating the dysrhythmias of the stomach is Enterra Therapy as mentioned earlier. This device is a non-rechargeable battery and it delivers current pulses to the tissue and this helps the stomach tissues to regain its rhythmic myoelectric activity. It also helps prevent the other symptoms like vomiting, nausea and abdominal pain caused due to Gastroparesis [1], [2], [3].

The design of wireless, batteryless, gastric stimulator has been demonstrated. The device harvests energy wirelessly so as to power a microcontroller and hence delivers electrical stimulation. Inductive coupling method is used to induce the current in the implant side. A series of wireless experiments have been conducted to demonstrate the feasibility of the stimulators. Chapter 4 discusses the experimental results in detail.

1.4 Thesis Organization

Chapter 2 describes the gastroparesis and the currently available different treatment methods. It also explains the currently available commercial gastro-stimulating device and its drawbacks. It also introduces the proposed wireless stimulator for Gastroparesis and its overall system design.

The complete wireless device design is introduced in Chapter 3. An overview of wireless power transfer is presented. This chapter also enlists the configuration of each block in the transmitter system and implant system. The system design for the transmitter circuitry, with design optimization techniques based on components characterization and

their results are described. The stimulator implant circuitry components are also explained in Chapter 3. A design of a radio frequency (RF)-to-direct current (DC) power converter including a bridge rectifier and LDO duo is presented. This chapter also provides the detailed description of both the models and detailed comparative study between various pulse generator modules used for the implant.

Chapter 4 consists of stimulator settings, the bench top experiments, initial tests of the implant circuitry and their experimental results. It also discusses the input and output characteristics of the wireless stimulator model and efficiency of different transmitter and receiver configurations. The reconfiguration of pulse setting is demonstrated in detail.

Finally, Chapter 5 summarizes the research results, draws conclusions, and outlines the future work. It mainly comprehends various models that can be considered in future of implantable gastrostimulator module. In future work fragment, the model for wearable transmitter is illustrated. At last, implementing the complete design on flexible substrate is explained.

CHAPTER 2

GASTROSTIMULATOR DEVICE OVERVIEW

2.1 Gastroparesis

Gastroparesis is a stomach syndrome in which the stomach takes very long time to empty its food contents. If food remains in the stomach for too long, it can cause problems such as bacterial overgrowth from the fermentation of the food. The food can also harden into solid masses, called bezoars, that may cause nausea, vomiting, and, sometimes, obstruction in the stomach. This can be dangerous if they block the passage of food into the small intestine. Figure 2.1 shows the peristalsis action of stomach muscles in pushing the food inside the small intestine. This action in case of gastroparesis is seized and it leads to many symptoms like nausea, fullness, anorexia, severe weight loss, abdominal pain, vomiting, and bloating. It is also associated with abnormal gastric myoelectric activity i.e. abnormal slow-wave frequency, low slow-wave amplitude, and slow-wave uncoupling [9]. This is also known as uncoordinated gastric or duodenal contractions [10].

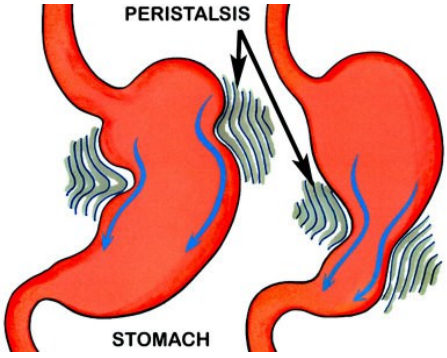

Figure 2.1 Peristalsis movements of stomach muscles

Gastroparesis can be caused by a number of factors and is commonly seen in patients with diabetic condition and often the cause is unidentified. Also it is more prominent among females than males. In North America alone approximately 5 million people including children suffer from gastroparesis. Many cases are obstinate and do not respond well to the drug based treatment. Gastroparesis is very difficult to treat and treatment options are very limited. There are few medications available, mostly aimed towards symptom control rather than dealing with the underlying problem. For this reason, they are often not effective.

2.2 Different Treatment Methodology

One of the most common and effective medication in treating gastroparesis is metoclopramide, which helps the stomach to empty by stimulating stomach muscle activity and it also may relieve nausea and vomiting. The common side effects of this medication include drowsiness and fatigue. In addition, some people may experience depression, movement disorders, anxiety and breast tenderness or discharge. Metoclopramide is not recommended for patients with Parkinson's disease.

The antibiotic erythromycin also helps in stomach emptying, but its side effects of nausea; vomiting and abdominal pains limit its usefulness. One additional drug called domperidone is not approved for use in the United States. Domperidone improves stomach emptying by stimulating stomach motor activity and relieves nausea and has few side effects. Additional new methods are being evaluated in studies. In extreme cases of gastroparesis, patients may need a semi-permanent intravenous (IV) line that delivers nutrients and fluids directly into the bloodstream.

In recent years the implant based method for treating gastroparesis has become more effective and more predictable in case of recovery progress. Gastric electrical stimulation is an implant based method and it uses a device, surgically implanted in the

abdomen, to provide mild electrical pulses to the nerves and muscle of the lower portion of the stomach. This stimulation reduces chronic nausea and vomiting. In this thesis much of the work is dedicated to improvising the implant method by addressing major issues in existing treatment techniques.

2.3 Gastric Electrical Stimulation (GES)

The associations between changes in electrical activity of gastric muscle, gastric emptying and symptoms led to the development of electrical stimulation models with the goal to entrain the rhythmic activity of the stomach, thereby regulating gastric function. GES is a therapeutic technique in which either high frequency/low energy (HFLE) or low frequency/high energy (LFHE) electric pulses are supplied to the stomach tissues for gastric emptying and regaining the normal stomach motility. Figure 2.2 represents a typical GES method and implant configuration. In earlier experiments, the current required for the stimulation varied from 2 to 6 mA [11], [12], [13], and the stimulators need to be functioning continuously or for long periods.

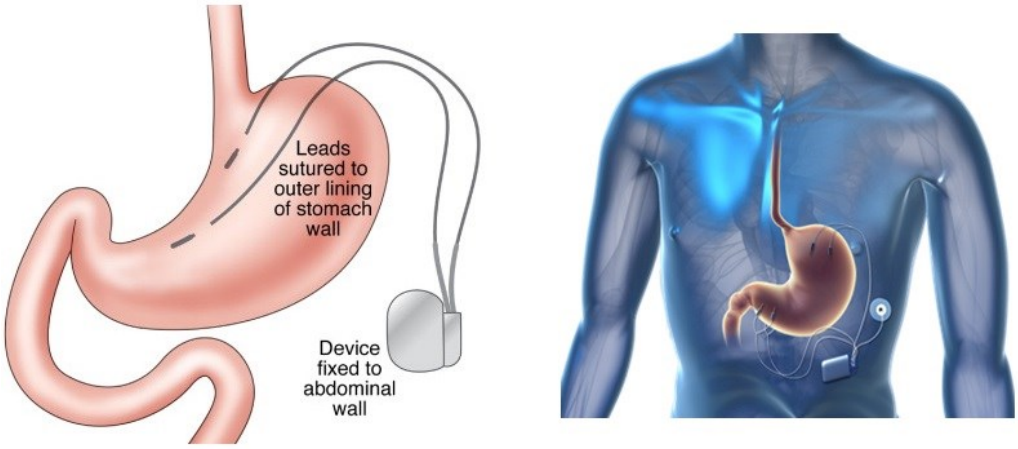

Figure 2.2 Gastric electrical stimulation (GES) and implant method

Providing power to the stimulators has thus become a primary design challenge for this implantable device. For fully implantable devices, the battery needs to be included

in the stimulator and as a result larger capacity battery is required. Since the device size is large, the surgical implantation with general anesthesia requires the patient to be eventually hospitalized. Currently, only one gastric electrical stimulator has received approval from the U.S. Food and Drug Administration (FDA), the GES system (now called the Enterra™ Therapy System), manufactured by Medtronic. This system consists of four modules: the implanted pulse generator, unipolar intramuscular stomach leads, the stimulator programmer, and the memory cartridge. With the exception of the intramuscular leads, all other components have been used in other implantable neurologic stimulators, such as spinal cord or sacral nerve stimulation. The intramuscular stomach leads are implanted either laparoscopically or during a laparotomy and are connected to the pulse generator, which is implanted in a subcutaneous (just beneath the skin) pocket. The programmer sets the stimulation parameters, which are typically set at an “on” time of 0.1 sec alternating with an “off” time of 5.0 sec. Figure 2.3 shows the actual stimulation device. This device dimensions are 60 mm x 55 mm x 10 mm, and it contains a non-rechargeable lithium-ion battery which has to be replaced each 2 to 8 years when it is exhausted [16], [17], [18].

Figure 2.3 Medtronic Enterra™ GES system (60 x 55 x 10 mm^3)

The objective of this project is to reduce the stimulator size and a novel device that does not contain any battery at all but can harvest electromagnetic energy wirelessly

to generate stimulation pulses. Wireless power transmission for medical applications has been studied by Schuder *et al.* who detailed the theoretical illustration. In their research inductive coupling between a pancake-shaped coils on the skin surface was used, that can transfer power efficiently to a coil placed inside the human body [21], Others such as Andren *et al.,* Meyers *et al.* and Newgard *et al.* have suggested of use ferromagnetic cores in inductive coupling for efficient transfer of magnetic energy through the skin [22], [23]. Wireless power transfer for medical devices can overcome many issues like contact failure, the need for replacing the battery each time it is exhausted and hence infection due to repeated invasive surgeries. However substantial power delivery to the implant is the biggest challenge for devices operating with inductive coupling. These devices generally have to be operated at a very short distance [24] due to limited power. Since then many medical applications have been demonstrated for transmission of energy in other medical applications such as neuron recording [25], pressure monitoring in stems and gastro-esophageal acid reflux sensing [27] applications. Many such applications are focused on providing energy into the body to operate sensors and power wireless transmitters to record the bio-potential signals. With the advances in low-power integrated circuits, the energy required to operate such devices are provided by inductive coupling and proved to be significant after following special methods. Magnetic fields through inductive coupling at low frequencies can penetrate deeper inside the human body without electromagnetic interference. However, delivering a significant amount of electromagnetic power to the implant still remains the main technical challenge.

2.4 Proposed Stimulation System

The proposed implantable gastrostimulator system consists of an external transmitter module and an implant tag module. The external coil transfers RF electromagnetic energy through the stomach tissues to provide the power required for the

implant to stimulate and stimulator generates electrical pulses and have protruded electrodes anchored into the stomach tissues. In practical scenarios, the stimulators will be implanted by either surgery which is the current implementation method for existing large stimulators or with an endoscope implantation which is non-invasive. The stimulator form factor needs to be reduced to very small scale so that they can be implanted by the endoscopic method. The miniaturization has been illustrated in the later chapters. The stimulation pulse trains were preprogrammed into an active controller and placed in the implant. In our experiments, three different stimulation settings (Low, Medium and High) were used. These settings were designed according to existing medical reports, using GES for gastroparesis treatment.

2.5 Discussions

After the detailed study on all the existing treatment methods available up to date for treating gastroparesis, developing a simpler solution appeared to be a vital need. It will be more beneficial to both society and the human community. In this work, development of miniaturized gastric electric stimulation device has been designed and developed. The design involves a completely wireless model without any battery. This device is operated at real time whenever RF electromagnetic energy is triggered externally to the implant through the transmitter. In this method, eliminating the battery eliminates the need for future implant replacement due to limited battery recharging lifetime.

Further miniaturization of the device was carried out to ensure that the device is capable of implanted through an endoscope. This will eliminate the need for a major surgery, general anesthesia and hospitalization as well and it will, also reduce the treatment costs.

CHAPTER 3

WIRELESS IMPLANT CIRCUIT DESIGN

3.1 Implant Configuration

The main objective of the implantable gastrostimulator in this thesis is to reduce the form factor, wireless coil design for reduced design and finally reconfiguration of the stimulator settings without any RF communication IC. The implant circuit was designed on a solder board initially with through-hole components and then finally on 2-layer printed wire board (PWB). A coil antenna with the inductance value of 7 μH was made from an AWG-24 magnet wire wound around the PWB (radial configuration). The use of a thicker magnetic wire will increase the maximum magnetic flux (ψ) linkage and also increasing the inductance per turn ratio. This will aggravate the magnetic flux, since it can be demonstrated in equation (3.1). Since, the thicker wire will restrict the flexibility appropriate gauge factor for the wire need to be determined. AWG-24 was chosen because of its moderate flexibility and for winding restrictions around the PWB board. Also switching to thicker wire would increase the implant size. For the endoscopically implantable stimulator the maximum permissible thickness is 8 mm and therefore 14 turns with AWG-24 was a suitable choice.

$$\psi = \frac{LI}{N} \qquad (3.1)$$

The operating frequency (f) is 1.3 MHz and was chosen since it has been observed in many previous works that the frequency range from 1-30 MHz is the best for

implantable medical devices. It also provides maximum permissible exposure (MPE) of magnetic field to the internal tissues.

3.1.1 RF to DC Conversion

In order to convert an RF signal into DC, the common method of converting AC to DC using a full bridge rectifier is used in this design. A bridge rectifier provides full-wave rectification from a two-wire AC input, resulting in lower cost and weight compared to a rectifier with a 3-wire input from a center-tapped transformer. In the past a Dickson charge pump has been used for RF to DC conversion but however considering the parasitics involved in that design due to more number of passive components (capacitors and diodes) the idea of using charge pump was ruled out. By selecting the fast recovery bridge rectifier the quiescent losses were minimized. Figure 3.1 shows typical bridge rectifier. In this design CMKBR-6F bridge rectifier from the central semiconductors is used.

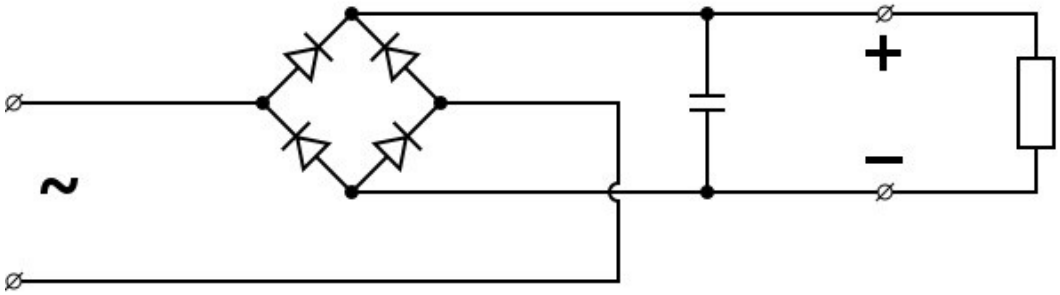

Figure 3.1 Full bridge rectifier circuit connected to regulator

The smoothing capacitor present in the input stage of the regulator converts the full-wave rippled output of the rectifier into a smooth DC output voltage. A capacitance of 1uF is used in between rectifier output stage and regulator input. However, there are two key parameters to consider when selecting a suitable smoothing capacitor. The operating voltage, which must be higher than the no-load output value of the rectifier and, the capacitance value which determines the amount of ripple that will appear superimposed

on top of the DC voltage. Too low a capacitance value and the capacitor has little effect on the output waveform. If the smoothing capacitor is sufficiently large enough and the load current is not too large, the output voltage will be almost as smooth as pure DC. As a general rule the have a ripple voltage should be less than 100 mV peak to peak.

3.1.2 Voltage Regulation

After the rectification, a constant DC regulation is required in order to run the controller which stimulates the stomach muscles periodically. There are two types of linear regulators: standard linear regulators and low dropout linear regulators (LDOs). The difference between the two is in the pass element and the amount of headroom, or dropout voltage, required to maintain a regulated output voltage. The dropout voltage is the minimum voltage required across the regulator to maintain regulation. A 3.3 V regulator that has 1 V of dropout requires the input voltage to be at least 4.3 V.

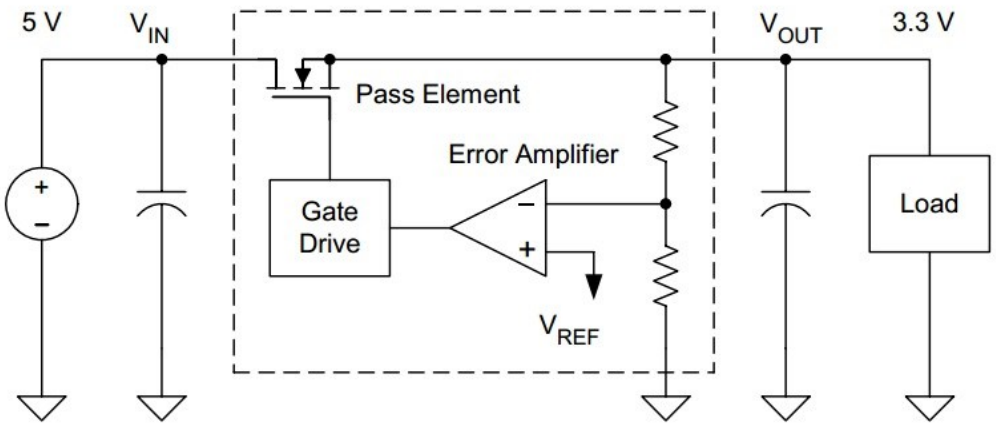

Figure 3.2 Internal drive circuitry of an LDO

Based on parameters such as static power consumption, wide range of input voltage and regulated output current, a Low Dropout Regulator (LDO) is chosen for voltage regulation. LDOs are a simple and inexpensive way to regulate an output voltage that is powered from a higher voltage input. They are easy to design with and use. The TI

LDO LM3480 was selected based on the input voltage range (30 V) and low quiescent current. The advantages of a low dropout voltage include a lower minimum operating voltage, higher efficiency operation and lower heat dissipation. Figure 3.2 shows the internal drive circuitry of a typical LDO. Before testing the rectifier and LDO on the prototype, both the components were tested on the breadboard level. Since the rectifier has a SOT363 package and the LDO has a SOT23 package, their corresponding Surface Mount Technology (SMT) to Dual-in-line (DIP) adapter is selected and tested on a breadboard level for different input voltage settings. The drop across the rectifier and the quiescent current of LDO is observed. Figure 3.3 shows the rectifier and the LDO soldered in the adapters.

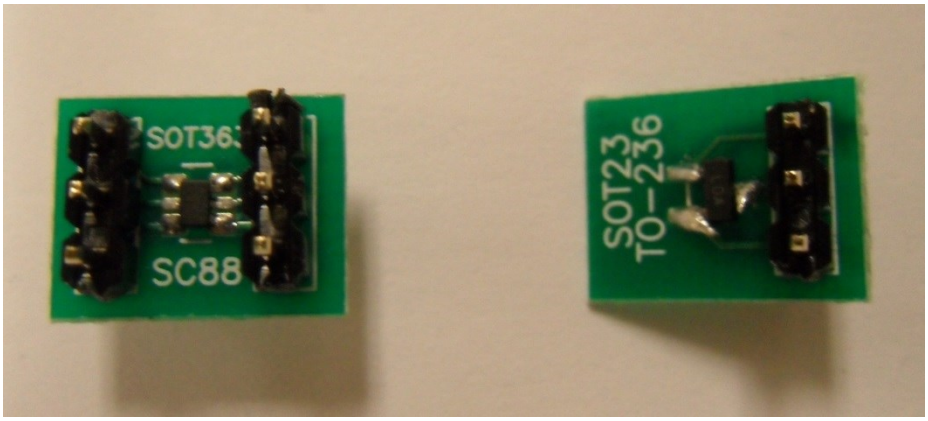

Figure 3.3 Bridge rectifier and LDO used in bench top experiment

3.1.3 PIC Stimulator

Peripheral Interface Controllers (PIC) series was chosen as stimulator for this application because it has a built-in oscillator with selectable speed and low power consumption. Especially PIC eXtreme Low Power (XLP) controllers [based on NanoWatt Technology] have very low power consumption and small form factor. Its sleep current is as low as 9 nA, active mode currents are down to 30 uA/MHz. Also it executes code smarter and maximizes the battery life. The Brown-out Reset (protects the device when

operating voltage reduces below minimum threshold value) current is down to 45 nA. Hence it protects when batteries are depleted or changed, and the timer current consumption is only 200 nA, it also provides protection against system failure. The real time clock consumes 500 nA, providing precise timekeeping. It comes with a DFN package, which has a form factor of 3x3x0.5 mm^3.

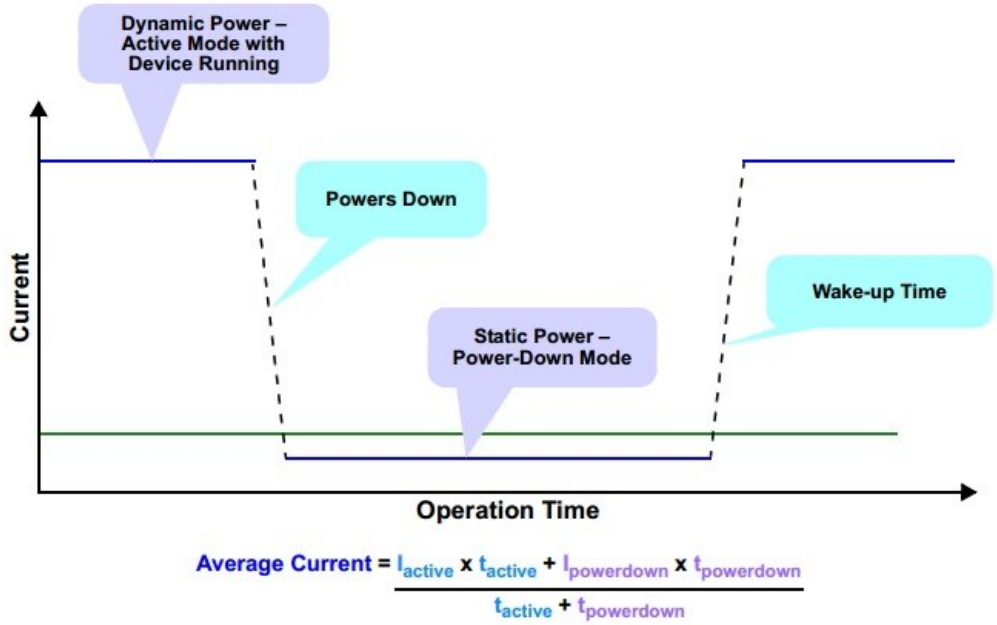

Figure 3.4 Method to estimate average current consumed by the stimulator

The selected controller is the PIC12LF1840 which is an 8 bit real time controller. The software program that is used to generate the pulse train for different stimulator settings is found in Appendix A. Based on the device active duration (with stimulating pulses) and device sleep mode duration, the average current consumed the stimulator can be estimated. Figure 3.4 shows the method to find the average power consumption.

3.1.4 Implant Block Diagram, Device Schematics, Layout and Form Factor

The implant system consists of a batteryless stimulator, an RF matching circuit to harvest RF electromagnetic energy into the body so as to power the stimulator, followed

by the rectifier and LDO duo. There is an additional block consisting of an attenuator and clamper in order to tap the transmitted signal to count the frequency. Based on this frequency information the settings are changed. In Chapter 4 the reconfiguration of gastrostimulator setting is discussed. The block diagram of the implant module is shown in figure 3.5.

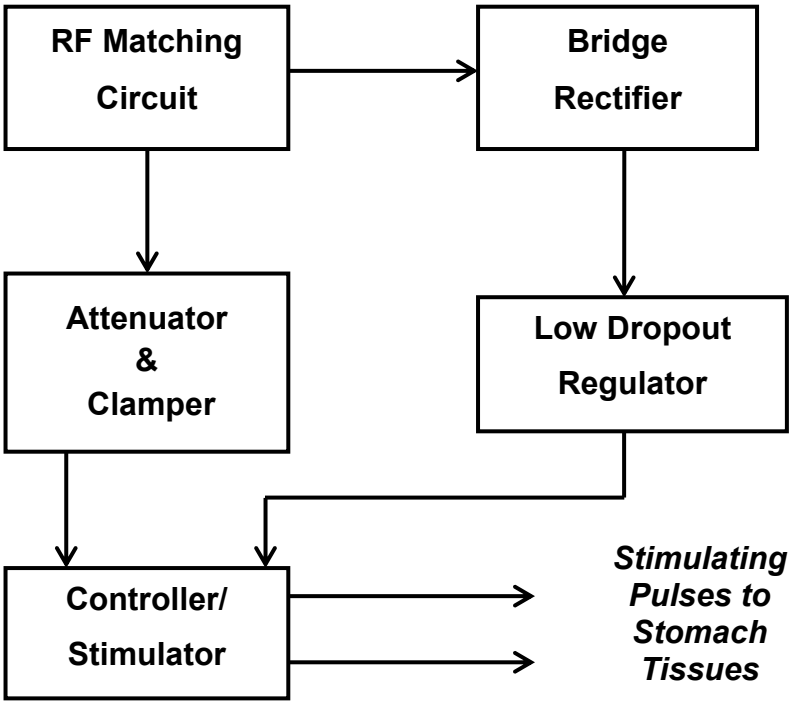

Figure 3.5 Block diagram of implantable gastrostimulator

The schematic entry of the complete implant circuit is drawn in the open source software called Eagle. Figure 3.6 shows the complete schematic diagram of the implant circuit design. The layout and PWB routing is performed with the same tool. With the two layers of PWB layout the overall dimensions of 13x7.2mm^2 is achieved. The overall stimulator layout is shown in Figure 3.7.

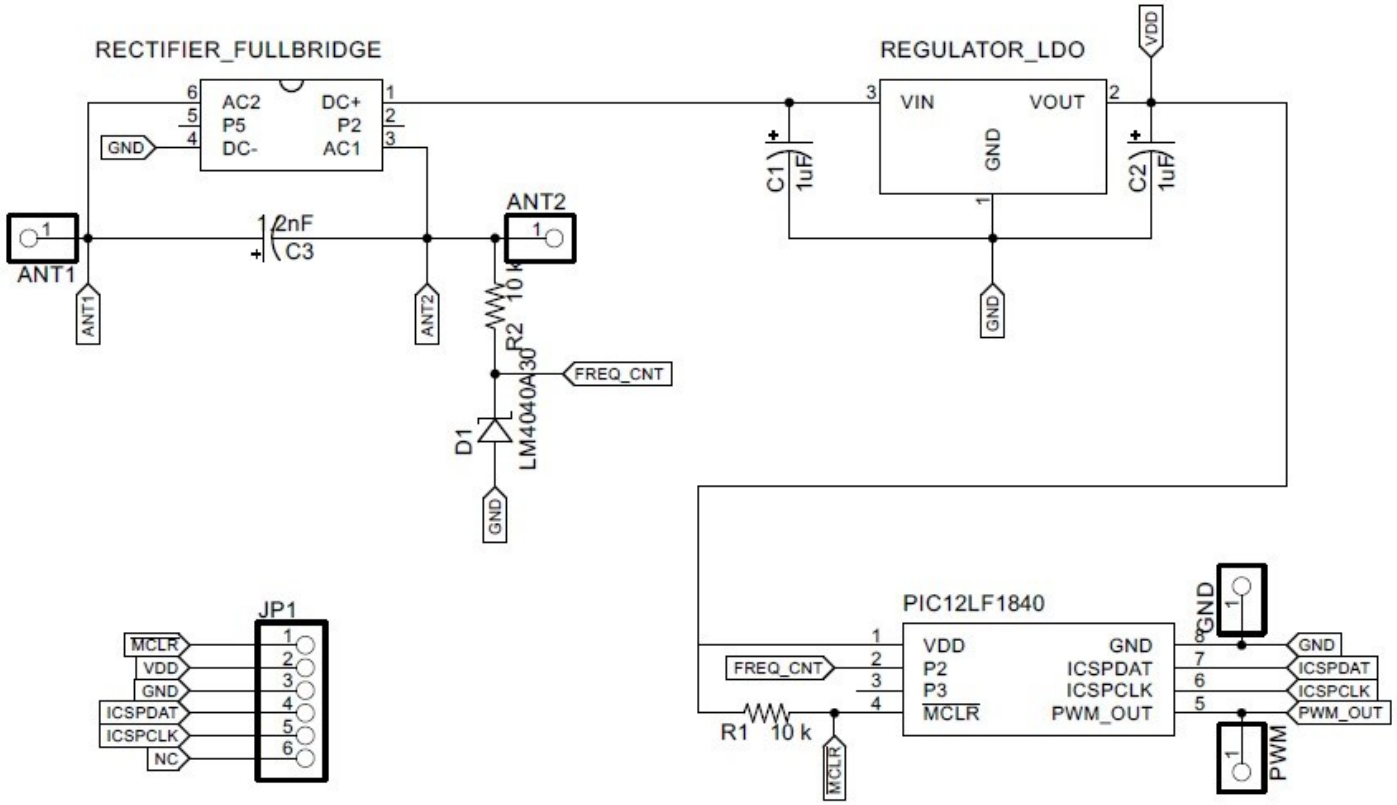

Figure 3.6 Schematic entry of the complete gastrostimulator circuit

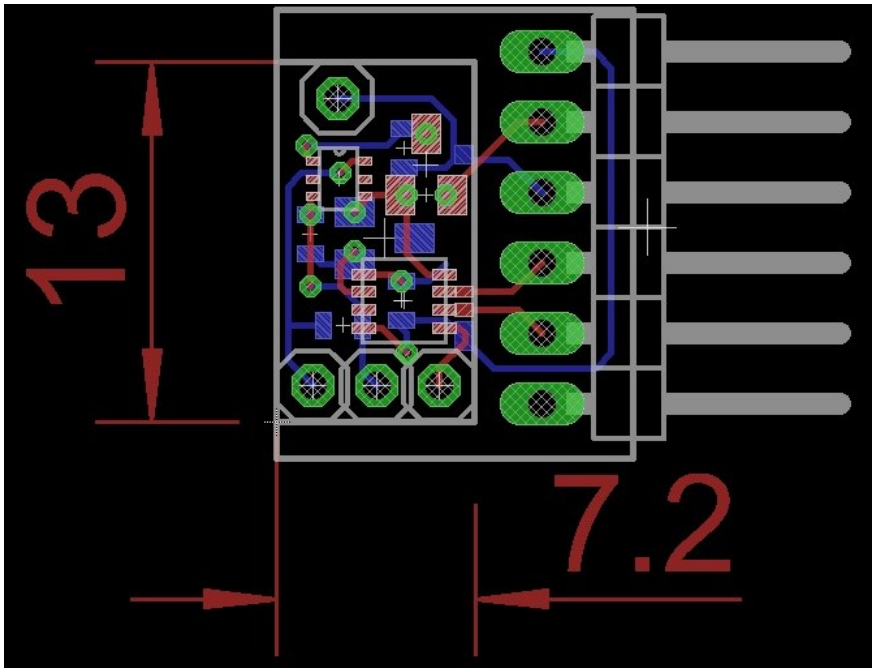

Figure 3.7 Final two layer PWB design of the gastrostimulator module (13x7.2 mm^2)

3.2 Transmitter Configuration

The transmitter module contains a coil antenna, signal generator circuitry, and a class-E amplifier resonating at the desired carrier frequency. The carrier frequency of 1.3 MHz is selected based on suggestions from previous studies for biomedical implantation applications that considered the transmission losses in the tissues. There is a good tradeoff between the voltage induced at receiver by inductive coupling and the carrier frequency chosen. When the frequency is increased the voltage induced also increases. However the losses at the tissues also increase with frequency. The coupling efficiency decreases as the frequency increases beyond 10 MHz for the biomedical implantable devices.

3.2.1 Class-E Amplifier Optimization

The class-E amplifier is a highly efficient switching power amplifier, typically used at such high frequencies that the switching time becomes comparable to the duty time. A

class-E power amplifier is selected, because in the ideal case the voltage and current of the amplifier would be 90° out of phase and hence the power consumption will be almost zero. The Class-E amplifier is also been considered for transcutaneous power delivery for numerous such applications in recent years. Other amplifiers such as class-A, B, AB, and C are either power inefficient or produce very high distortion, though their structure is not very complex. Class-D amplifiers also contain many harmonic spectral components. The carrier frequency is generated using a function generator with an amplitude of 6 V peak to peak. Both radial and spiral transmitter coil antennas with a radius of 5 cm were made from AWG-24 wires. A quality factor (Q) of 80 and an inductance (L1) of 64 μH were measured. A MOSFET (IRF510 from Fairchild Semiconductor) is selected for the class-E amplifier based on its low threshold voltage.

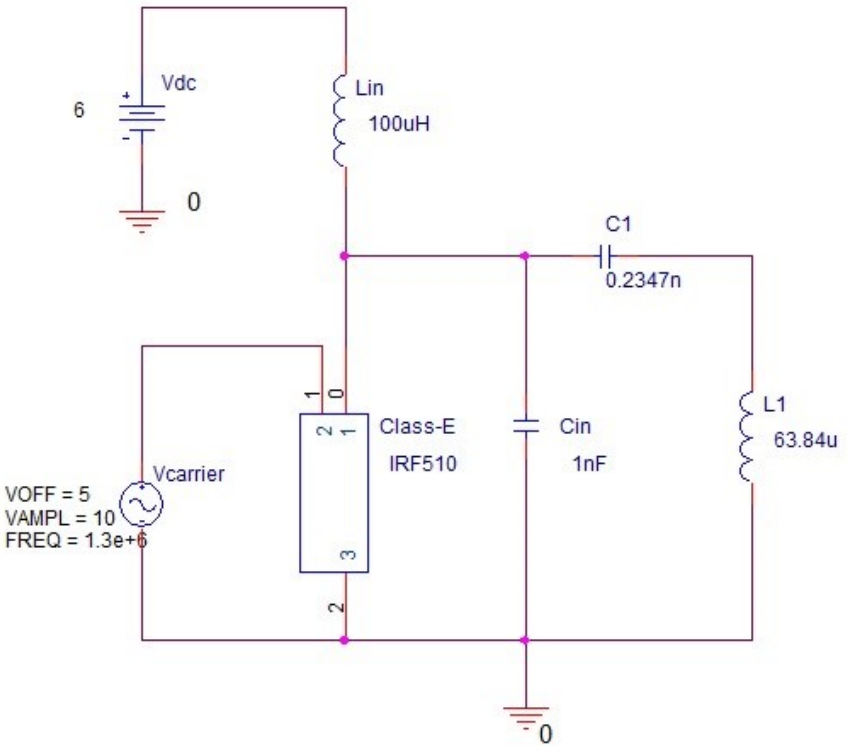

Figure 3.8 Class-E amplifier schematics with transmitter circuit

The inductor L in the class-E amplifier acts as a current source which is connected to the 6 V power supply and provides the current to the resonant circuit. The tuning capacitance C1, of 150 pF is chosen to resonate the circuit at 1.3 MHz and a shunt capacitor Cin of 10 nF was used for discharging. Resonance with high-Q is a very important for maximum power transmission through the class-E amplifier and the transmitter antenna. The equivalent circuit diagram of the transmitter that was simulated in PSPICE is shown in figure 3.8.

3.2.2 Wireless Transmission Efficiency Optimization

To maximize the power transfer through an inductive link, optimization procedures for the transmitter antenna were carried out. In these experiments, the main variables to be optimized are number of turns of the transmitter coil for a particular coil gauge and the transmitter size. To obtain an appropriate number of turns and size of the transmitter a series of calculations and experiments were performed. In Section 4.2 wireless power transfer experimental results are discussed.

3.3 Antenna Design

The antenna design plays a significant role in implant device operation. One of the major focuses was on the power transfer efficiency with different antenna configurations. The reduced antenna size at the implant size will make endoscopic implantation much easier. Also, the power coupled to the implant module as the function distance needs to be investigated to make the device operate above threshold level. Figure 3.9 shows the equivalent circuit for wireless power transfer. In order to provide sufficient wireless power to the implant, the study of energy scavenging efficiency in air targeting a distance of 4 to 9 cm is performed. The loss through similar tissue thickness was about 50%. The constraining factors included the small sizes of coil antennas and limited transmission RF power. The goal is to achieve optimal power transfer efficiency.

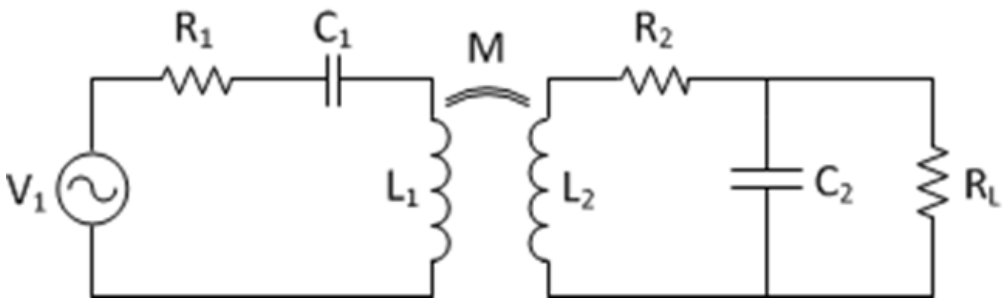

Figure 3.9 Equivalent circuit of wireless power transfer

3.3.1 Transmitter Coil Configuration

The transmitter tested in this project has two different configurations. One is radial and the other is spiral. Based on the previous research work on the coil antenna design, it is suggested that 5 cm radius is optimum for a wearable module. Since the patient has to wear the transmitter module around his waist or through the jacket the overall size should as small as possible, and at the same time it has to have enough power delivering capability to the implant coil. Figure 3.10 shows the radial and spiral transmitter coil used in this project.

In this design the transmitter antenna is made with AWG-24 copper wires of 5 cm radius for both the radial and spiral winding configuration. Earlier experiments [28] showed that the 5 cm radius antenna in general consumed lower input current and had a lower inductance so the matching capacitance would be sufficiently large to tolerate changes in parasitics capacitances in the environment preventing the resonance frequency from shifting. Having optimum size of transmitter antenna will be easy and more comfortable for the patient to wear. Between the radial and spiral transmitter antenna configuration, the spiral antenna induced more current in the implanted circuit. The efficiency was more than 10 times that of a radial coil. The following figure shows the comparison between the spiral and the radial transmitter coils. Based on all the

experimental results, the spiral transmitter antenna and 14 turn AWG-24 wire radial coil at the implant side is chosen.

The transmitter circuitry and Li-ion battery packs are very small. Hence the transmitter antenna dimension determines the size of the wearable module. So, the size of the primary coil is limited to 5 cm in radius for the patient's comfort. In addition, the resonant capacitance C_1 fell below 100 pF when the total length of the primary coil was around 600 cm, which resulted in 17 turn coil with a radius of 5 cm.

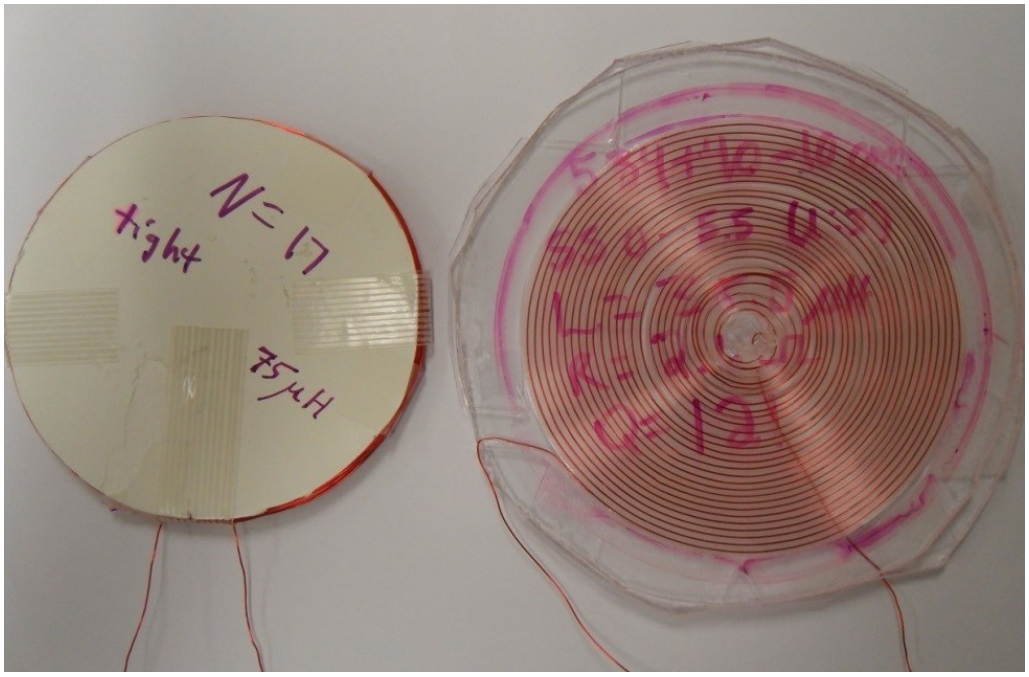

Figure 3.10 Radial and spiral transmitter coil

3.3.2 Tag Coil Configuration

The implant dimensions that was obtained from the PWB layout is used to define the coil antenna dimensions as 1.3×0.7 cm^2 as shown in figure 3.11. The metal wire was wounded around the rectangular-shape PWB to maximize its aperture size. The coil wire is connected to the tuning capacitor, followed by a voltage rectifier and low drop out regulator. The number of turns of the coil antenna and the metal wire gauge were limited

in order to limit the thickness of the package so that the implant can be delivered through an endoscope. We chose AWG-24 wire with a tradeoff between unit-length resistance and wire thickness. Output power and efficiency were obtained for 10, 12 and 14 turn implant coil, based on the implant current requirement 14 turn configuration is selected.

Based on the above selected tag antenna configuration the inductance was obtained from an impedance analyzer and found to be 7.2 uH and the corresponding matching capacitance for 1.3 MHz is 3.5 nF. The resonant frequency for LC parallel circuit is used from the equation 3.2.

$$f_s = \frac{1}{2\pi}\sqrt{\frac{1}{L_S\, C_S}} \qquad (3.2)$$

L_s - Inductance of the Sensor

C_s - Capacitance of the Sensor

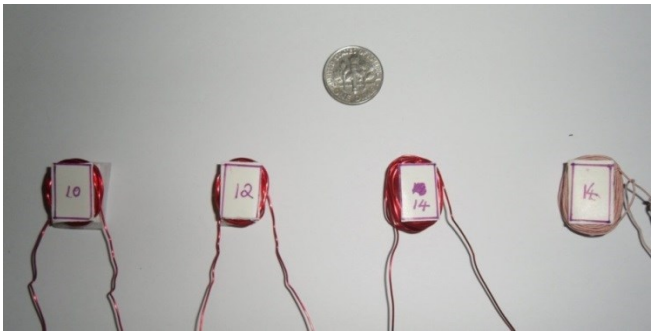

Figure 3.11 Implant receiver coil with different configuration

Since most of the parameters in the implant are fixed, the primary coil resistance, R_1, and the mutual inductance, M, determines the transfer efficiency. The mutual inductance is determined by equation (3.3) and the coupling coefficient, *k*, can be found from the coil antenna shapes, sizes, and distances between the coils.

$$M = k\sqrt{L_1 L_2} \qquad (3.3)$$

With inductance, L_2, fixed the variation in *M* with inductance, L_1, is investigated for different distance of separation between transmitter and receiver module. The output power and efficiency as the function of distance is obtained.

3.3.3 Experimental Setup

To fairly carry out the wireless power transfer experiments, a wooden box with slots at fixed distances were used to measure the receive power at different distances as shown in figure 3.12. Also, the experiment was repeated for a different number of turns at the receive tag antenna.

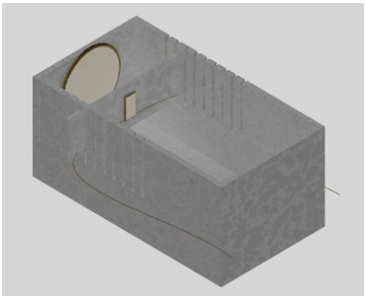

Figure 3.12 Setup used to carry out wireless power transfer experiments

The mutual inductance was measured with the open-short method for each transmitter and implant coil pairs [71]. An n-channel power MOSFET (Fairchild, IRF510) was used in the class-E amplifier to amplify the 1.3 MHz carrier signal fed by a function generator with 6 V pulse signal, with a 50% duty cycle, and with an offset of 3 V dc.

The output voltage was measured on the load resistor for output power while the input voltage and current were measured to obtain the input power. The overall power transfer efficiency obtained from the experiments results are discussed in Section 4.2. A method of measuring low to high gate drive transition was used to obtain the efficiency of the class-E amplifier. The complete experimental setup is shown in figure 3.13.

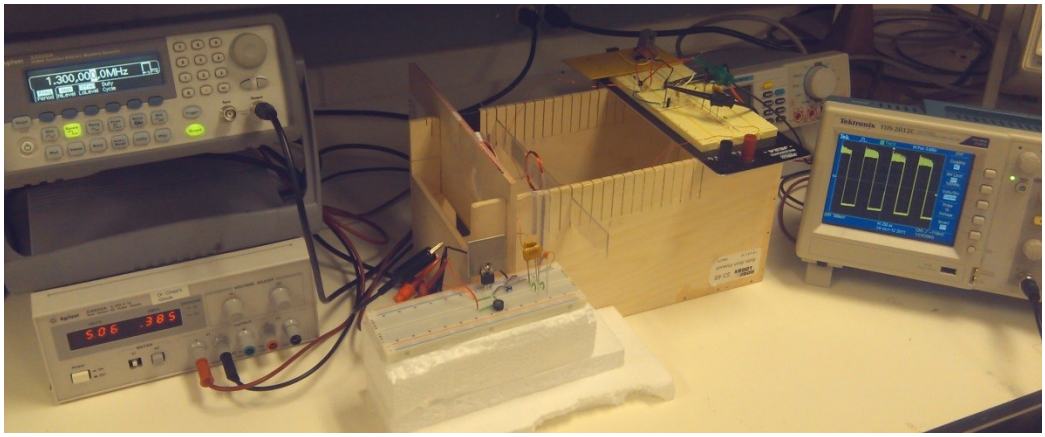

Figure 3.13 Experimental setup of wireless power transfer

3.4 Summary

The main transmitter circuitry was designed with 17 turn 5 cm radius, which produced maximum voltage at the implant coil of the given size. Based on the experimental results AWG-24 wire with 14 turns is chosen for the receiver. Increasing the number of turns by more than 14 turns increased the efficiency, but it did not increase the efficiency as significantly as compared to the aggravating bulkiness of the whole device due to the increment of the number of turns. The main intention was to keep the transmitter smaller and lighter so that it could be worn by the patient as a belt.

The wireless power transfer via inductive coupling for implantable devices has been demonstrated by investigating parameters such as the number of coil turns, antenna configurations, and load variation and distance. Also, wireless power transfer issues in terms of output power and input power consumption as well as the transfer efficiency were discussed in this project. A system with low power consumption and high efficiency can achieve endoscopically-implantable miniature batteryless/rechargeable wireless devices for gastro stimulator operated by a wearable and portable reader. For a portable transmitter, an antenna could draw less current and should be more suitable.

However, a large sized antenna has less immunity against parasitic effects due to its high inductance. With these results, the radius of a 5 cm was found to be the optimal size.

CHAPTER 4

EXPERIMENTAL RESULTS

4.1 Stimulator Results

The pulse train parameters are illustrated in table 4.1 and the pulse setting is defined in figure 4.1. Three different stimulation settings, based on previous works were implemented in this stimulator design as shown in figure 4.2 and figure 4.3. Pulse frequency is defined within cycle "on" time period, T_{on}, and N is the number of pulses during the cycle "on" period, T_{on}. These settings were recommended based on the low, medium and high dosage needed to retain the stomach motility. Higher settings have faster pulses and lower T_{off} time. T_{off} represents the "off" period between each cycle of stimulation while T_o shows the "off" period between each pulse.

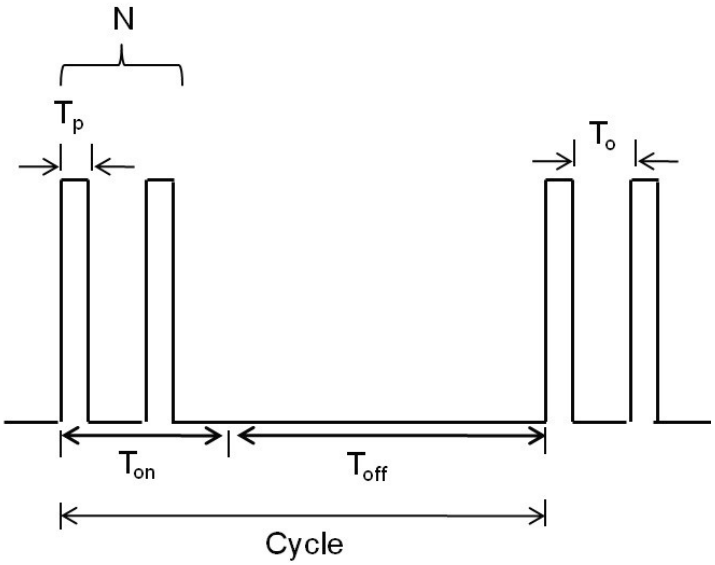

Figure 4.1 Pulse train definition

Table 4.1 Pulse and cycle specifications for the gastrostimulator

	T_p	T_o	T_{on}	T_{off}
Low	330 µs	14 Hz/71.4 ms	0.1 s	5 s
Medium	330 µs	28 Hz/35.7 ms	1 s	4 s
High	330 µs	55 Hz/18.2 ms	4 s	1 s

The NI-6210 DAQ card was used to capture the generated pulse train from the stimulator and the pulses are plotted using LabVIEW signal express. Two channels were programmed to record the pulses from the stimulator. A sampling rate of 100 ks/s was assigned. Figure 4.2 represent DAQ bench top setup.

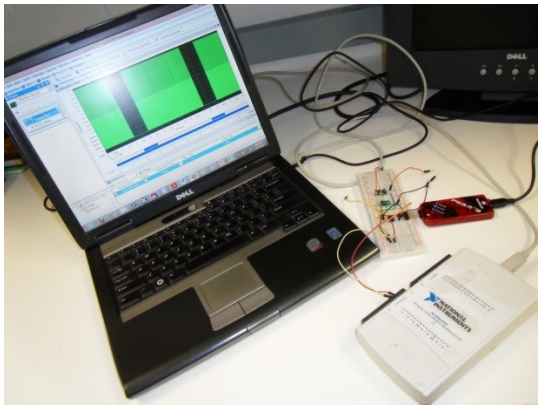

Figure 4.2 Data acquisition using NI-6210 DAQ card

Figure 4.3 to 4.5 represents the individual pulse duration of each setting. These pulses are generated using Pulse Width Modulation (PWM) module present with in the controller. The generated pulses are superimposed with the timer output to achieve T_{on} and T_{off}. The controller operates at 1MHz internal clock oscillator. As shown in figure 4.6 each cycle operating in the Low setting incorporates 2 pulses in 0.1 s with a period of 5.1 s, Medium setting includes around 30 pulses in 1 s ON time with a period of 5 s, while High settings includes approximately 220 pulses in 4 s of ON time with a period of 5 s.

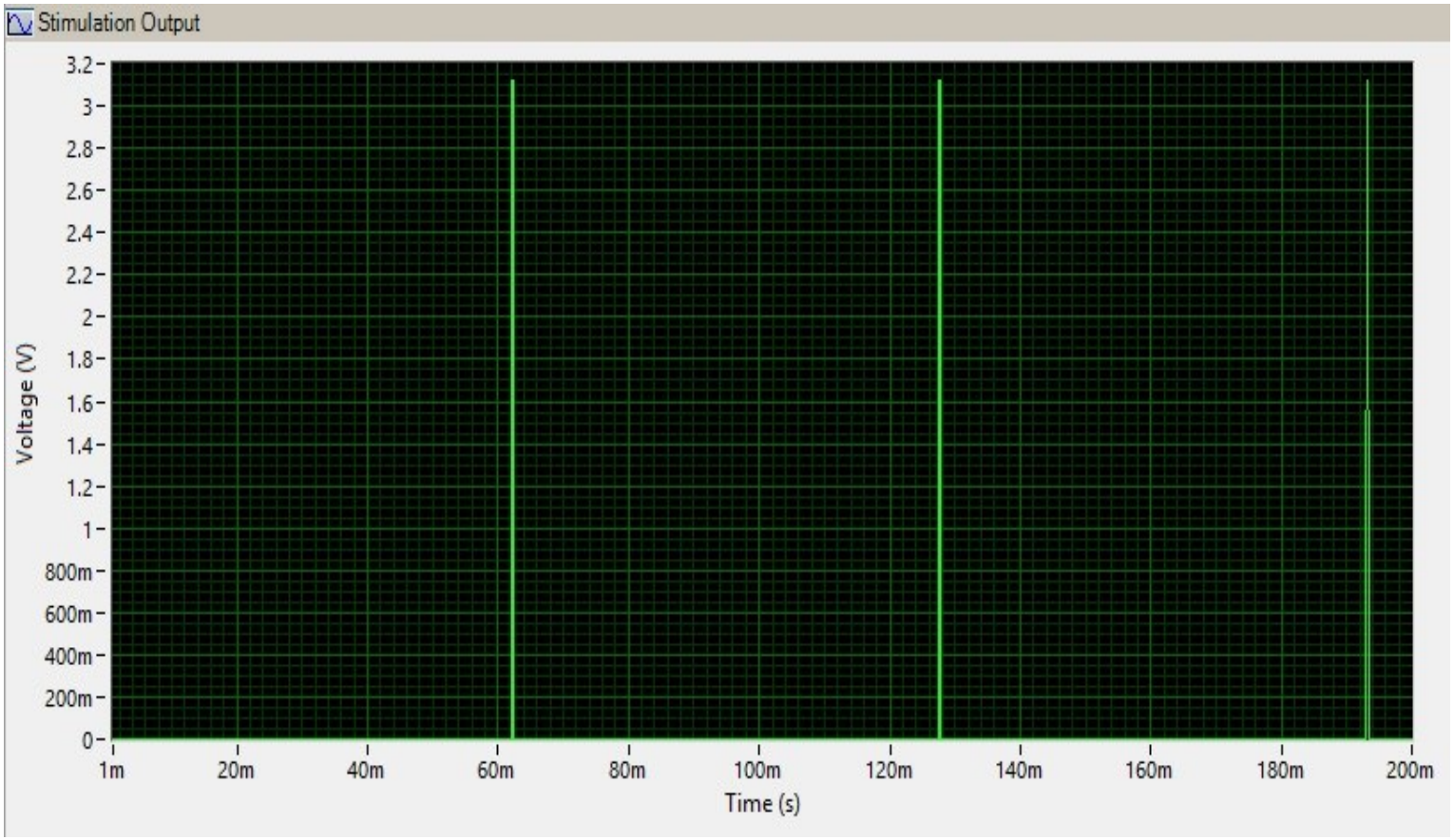

Figure 4.3 The Tp and To of low setting

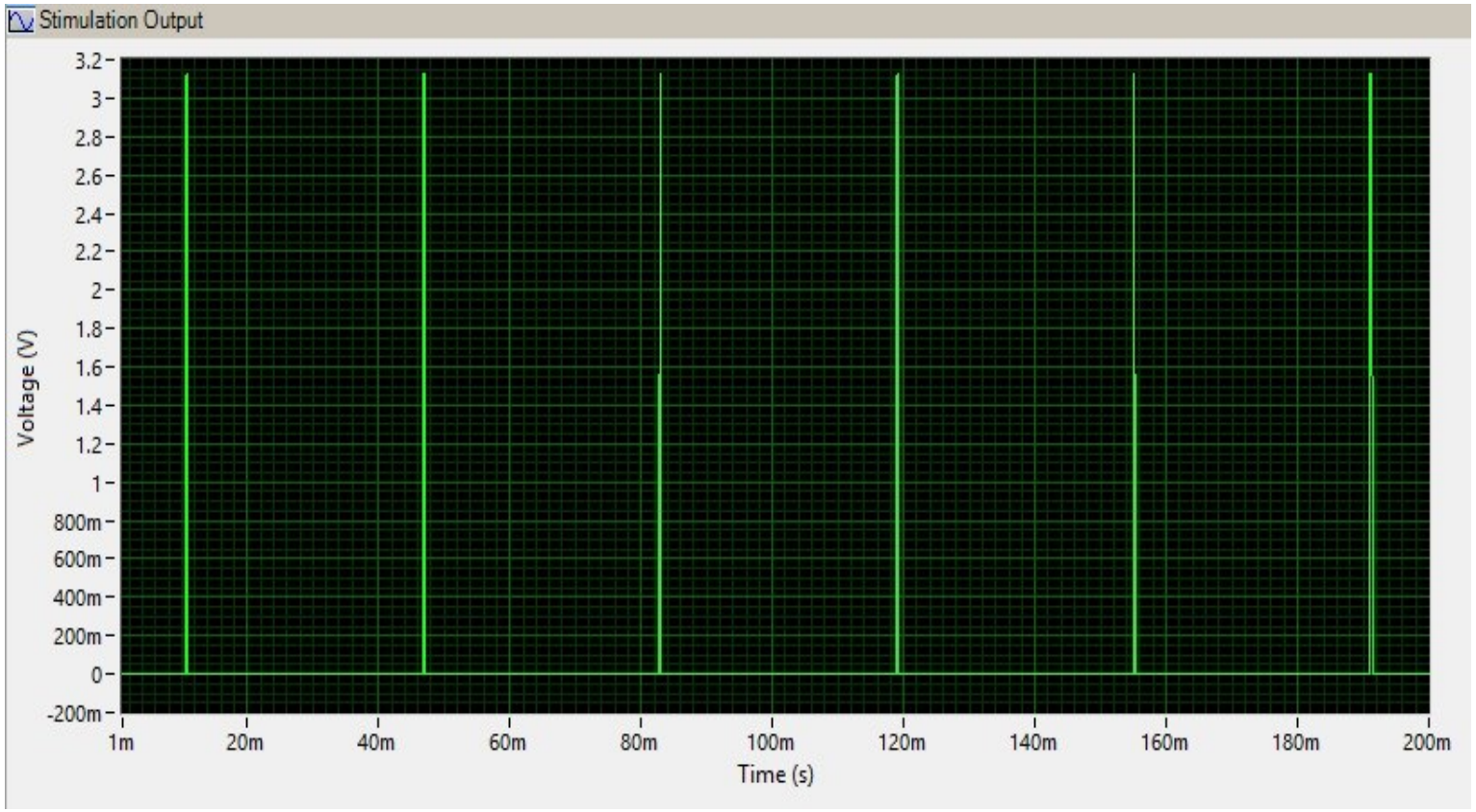

Figure 4.4 The Tp and To of medium setting

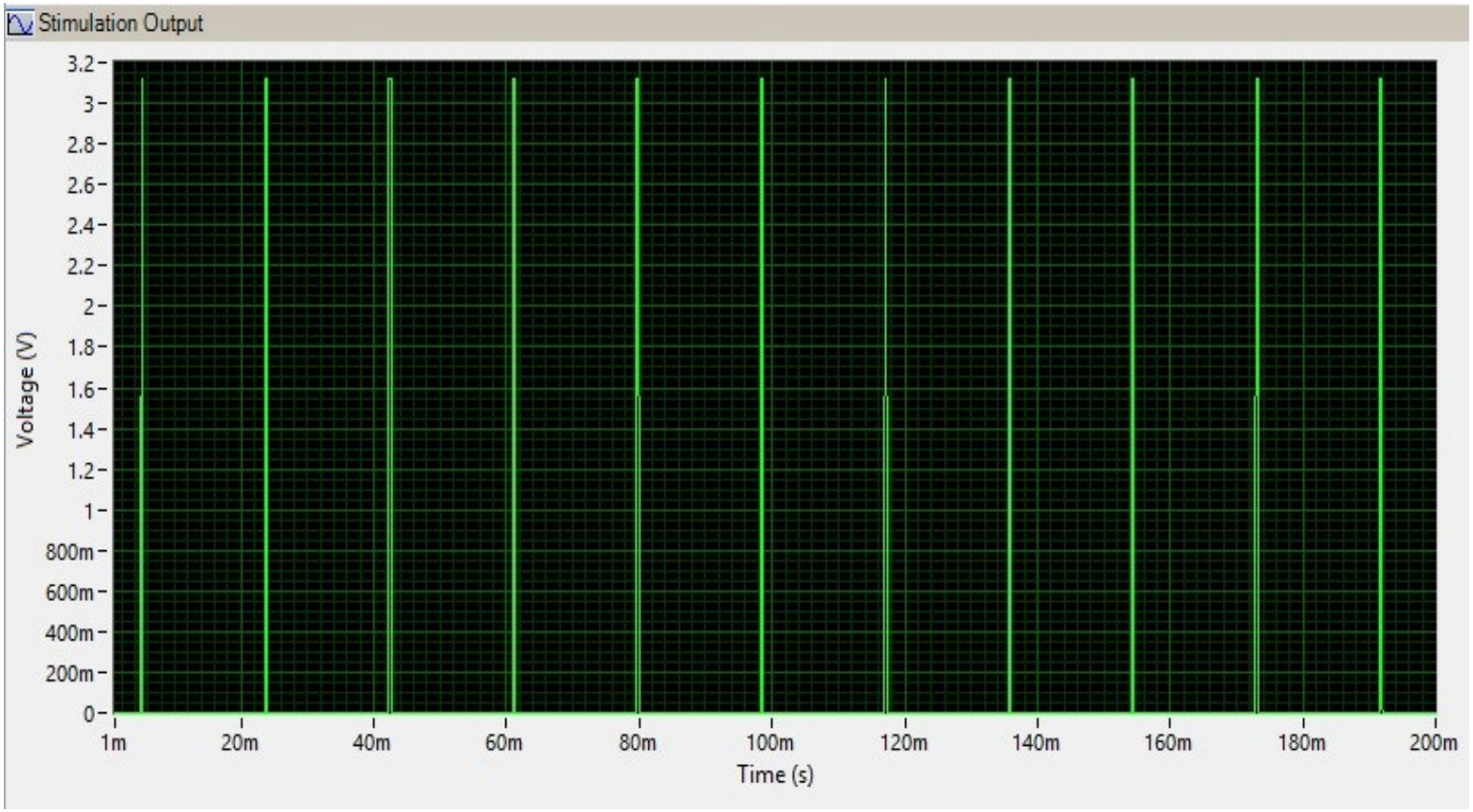

Figure 4.5 The Tp and To of high setting

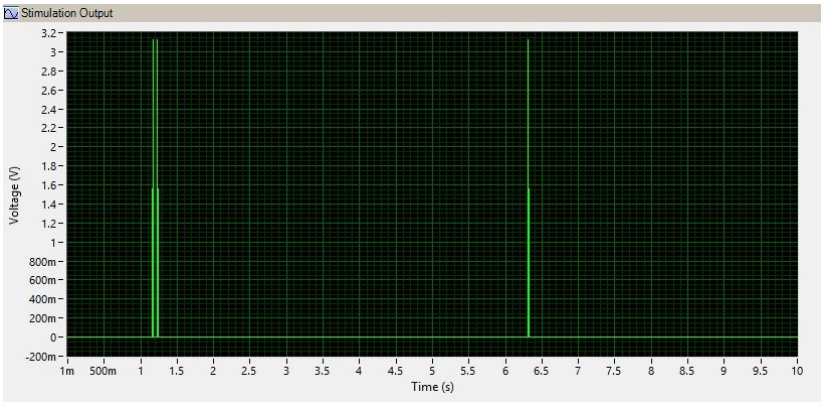

(a)

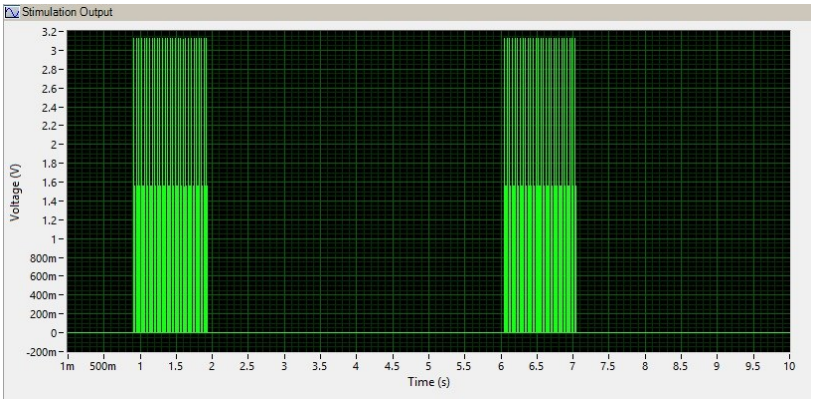

(b)

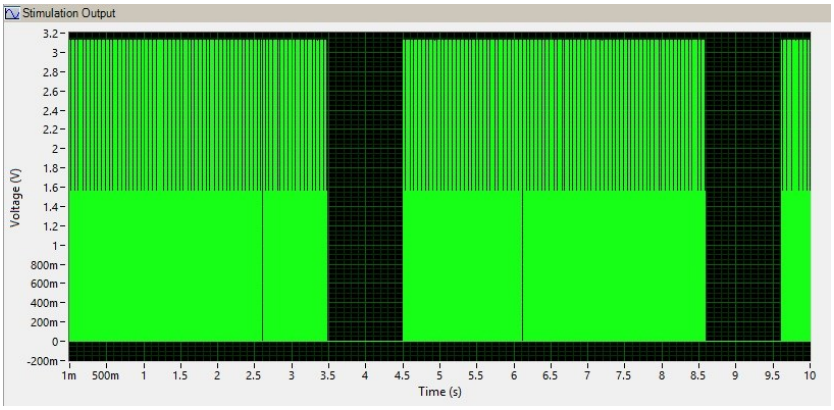

(c)

Figure 4.6 Generated pulse (a) Low setting (b) Medium setting and (c) High setting

4.2 Wireless Experiment Results

The wireless power transfer experiments play very important role in this project. In order to find the optimum design configuration and parameters, at the transmitter side radial and spiral coils were tested and at the implant side AWG-24 wire coils, and litz wire coils in radial configuration were tested as discussed in Section (3.3). In this section the input and output characteristics of the wireless system is discussed and finally the wireless power transfer efficiency for different configurations are plotted.

4.2.1 Input and Output Characteristics

The wearable transmitter module consists of rechargeable lithium ion battery. In order to estimate the endurance of the battery and to increase the period between consecutive recharge, series of experiments were carried out by changing the input dc voltage of the class-E amplifier. The spiral and radial configurations were tested at the transmitter, and at the receiver both AWG-24 wire and litz wire are tested with radial configuration. Figure 4.7 to 4.9 shows the input voltage versus output current through 500 ohm load for all the different configurations. From the data, it is clearly evident that spiral transmitter coil induces more current than radial coil even at very small input dc voltage. At the implant side, compared to litz wire the AWG-24 wire receives more current.

From these experiments, it is concluded that spiral transmitter coil and AWG-24 coil in radial configuration at the receiver side is the most optimum choice.

The output power obtained at different distances between transmitter and receiver is plotted in figure 4.10. It is clearly evident from this plot that spiral transmitter coil with AWG-24 coil at the implant can operate up to 9 cm and also well above the threshold levels. The other two configurations have very short range of operation.

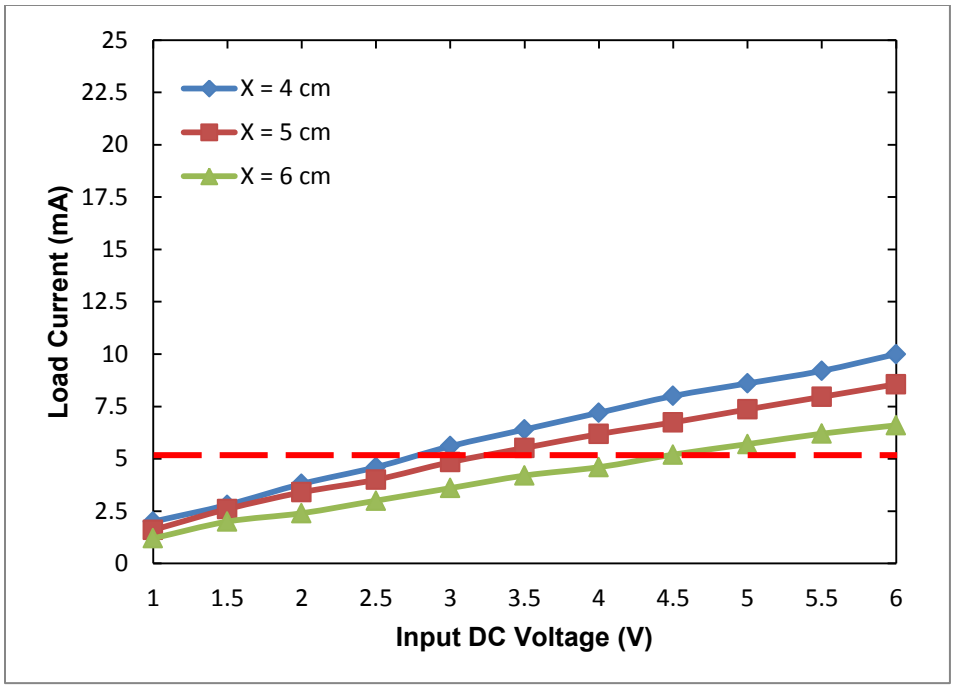

Figure 4.7 Transconductance plot for radial transmitter and AWG-24 wire at the receiver

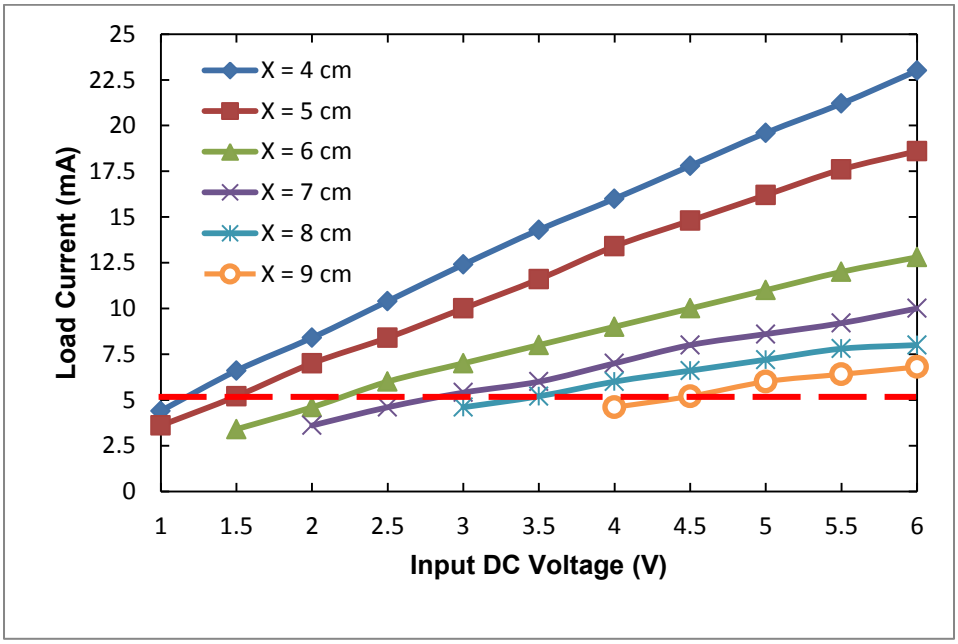

Figure 4.8 Transconductance plot for spiral transmitter and AWG-24 wire at the receiver

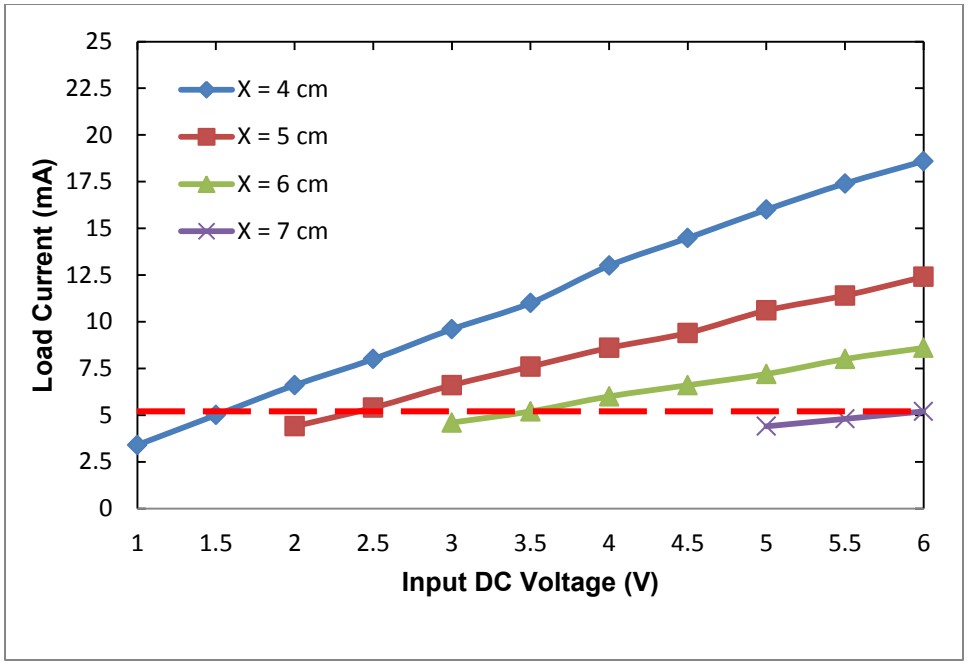

Figure 4.9 Transconductance plot for spiral transmitter and litz wire at the receiver

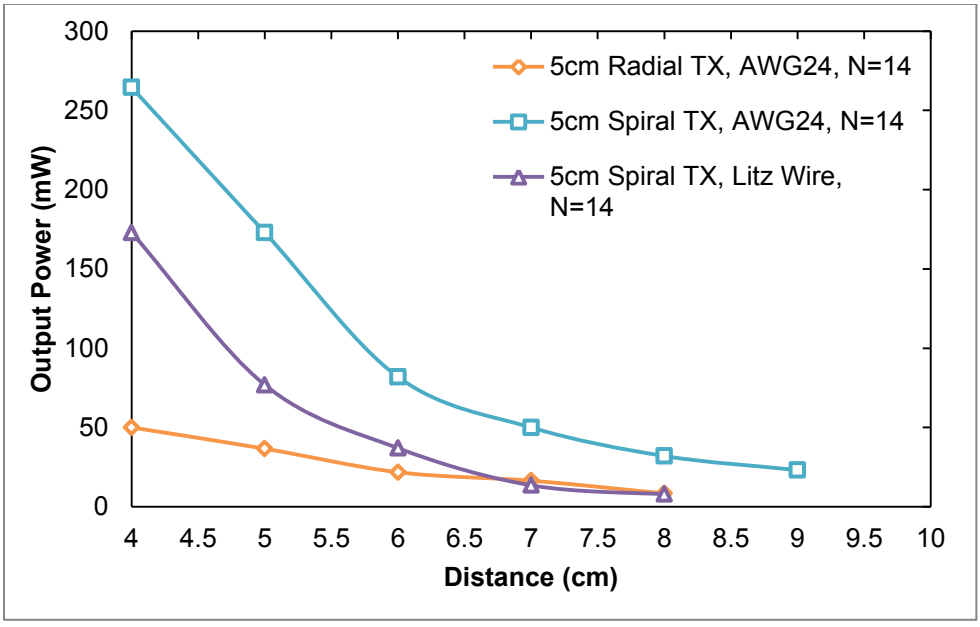

Figure 4.10 Output power vs. distances from the transmitter for all three configurations

4.2.2 Wireless Power Transfer Efficiency

The required number of turns for the implant coil is found by investigating with different turns in the experiment. Starting with 10 turn and all the way to 16 turn is tested. Since 16 turn exceeded the maximum thickness allowed for the stimulator and it also received more current which is very high for the device to withstand, 14 turn is set as upper limit. After testing the 10 turn, 12 turn and 14 turn at the implant side, 14 turn coil was found to be the best choice.

The 14 turn coil showed very high efficiency even at 9 cm. The output current was well above threshold level and also, the device thickness didn't exceed the maximum allowed size. This experiment was carried out with both the radial and the spiral transmitter coil. Figure 4.9 and 4.10 shows the efficiency of the receiver coil for the radial and the spiral transmitter coils respectively. Figure 4.11 shows the efficiency of 14 turn AWG-24 wire and litz wire receiver coil for both radial and spiral transmitter coil.

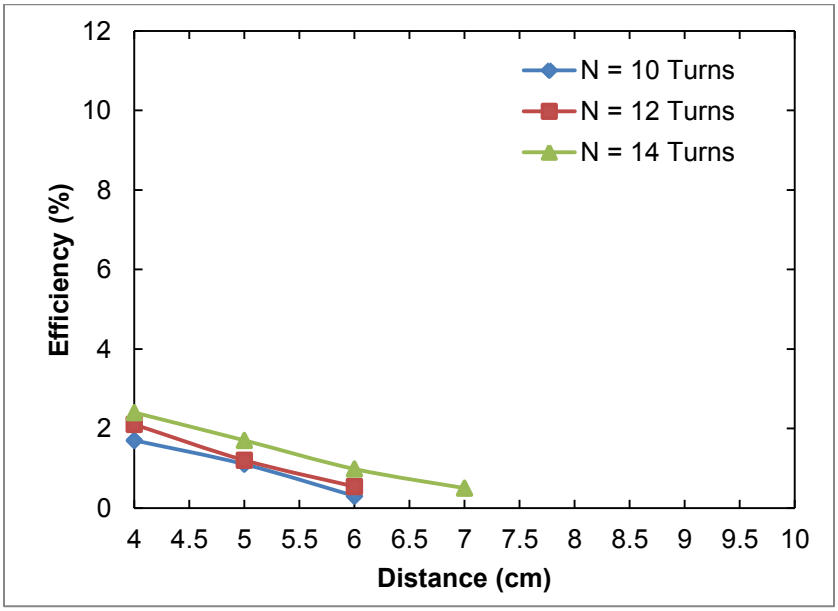

Figure 4.11 Efficiency of receiver coil with different turns and radial transmitter coil

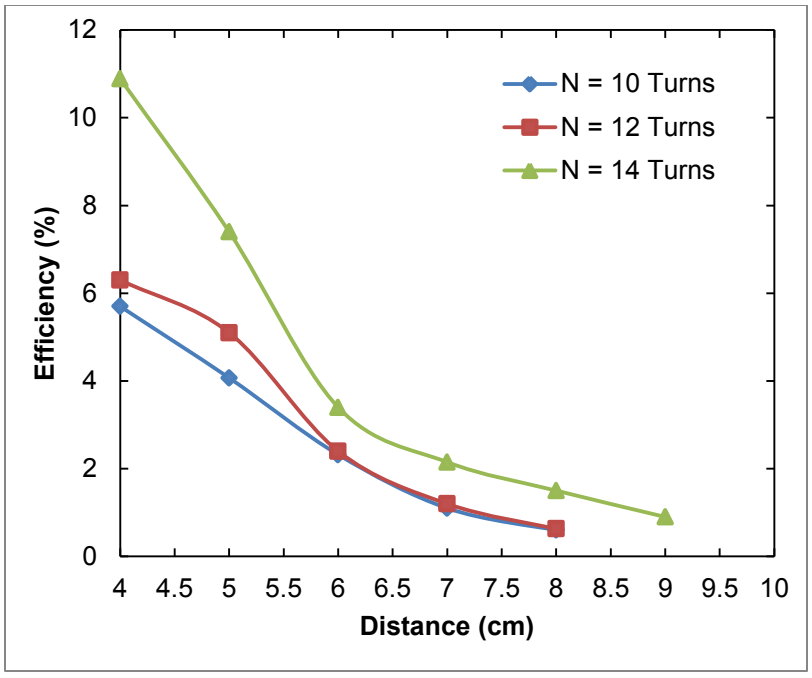

Figure 4.12 Efficiency of receiver coil with different turns and spiral transmitter coil

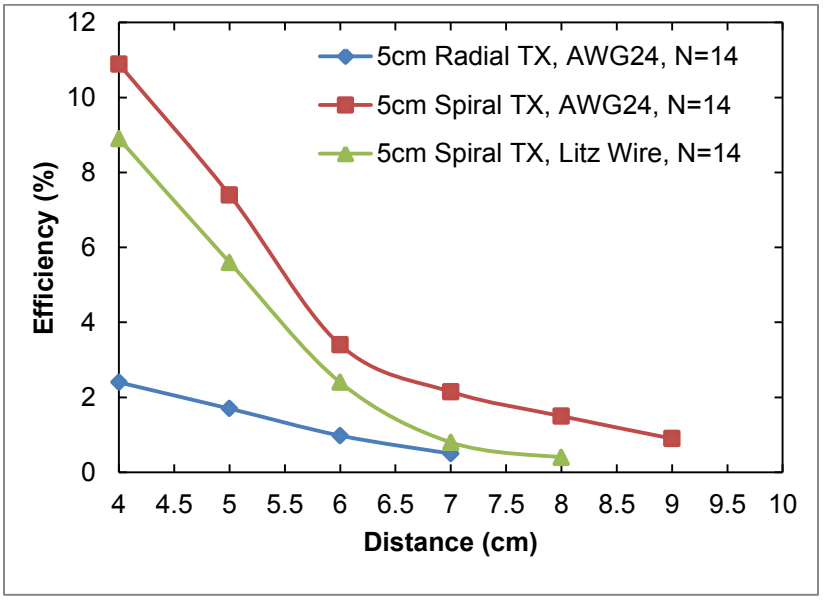

Figure 4.13 Efficiency of 14 turn coil with radial and spiral transmitter coil and AWG-24 wire and litz wire at receiver coil

4.3 Reconfiguration of Gastrostimulator Setting

The main objective of this section is to change the pulse settings after the device is implanted without involving any invasive surgery. In the past dedicated wireless communication module is used to change the pulse settings. The drawback of using radio module for changing the setting is it consumes additional power and it also increases the size of the implant module. Currently available RF IC requires at least 12 to 15mA of current in order to transmit and receive the data. Since this device is wirelessly powered, we have huge constraints on current consumption. Hence a new technique of using the frequency of the transmitted signal for wireless power harvesting, the change of pulse setting is performed. The method of frequency counting is used to count the carrier frequency. By configuring one of the timers in the controller in counter mode, the incoming frequency is counted. Since the frequency of the transmitter cannot deviate much from the resonance, a very small bandwidth is used for this reconfiguration. The frequency counting was very precise up to four decimal places. The resolution of the counter was approximately 2 KHz. Since we had enough bandwidth around the resonant frequency 1.3 MHz, this resolution was well above the requirement.

From the above plot shown in figure 4.12 in the frequency band of 1.32 MHz to 1.36 MHz, the output voltage across the load is above the threshold levels. Hence, by changing the transmitter frequency with in this bandwidth, the stimulator settings can be changed by counting the frequency precisely. Before changing the setting at the stimulator, the frequency is counted ‘N’ times and averaged it in order to prevent any faulty reconfiguration. In bench top experiments, the actual counted and averaged value is verified by reading the stimulator settings using UART and serial communication

module. Figure 4.13 shows the block diagram of frequency counter module and resolution of the counter for different set of frequencies.

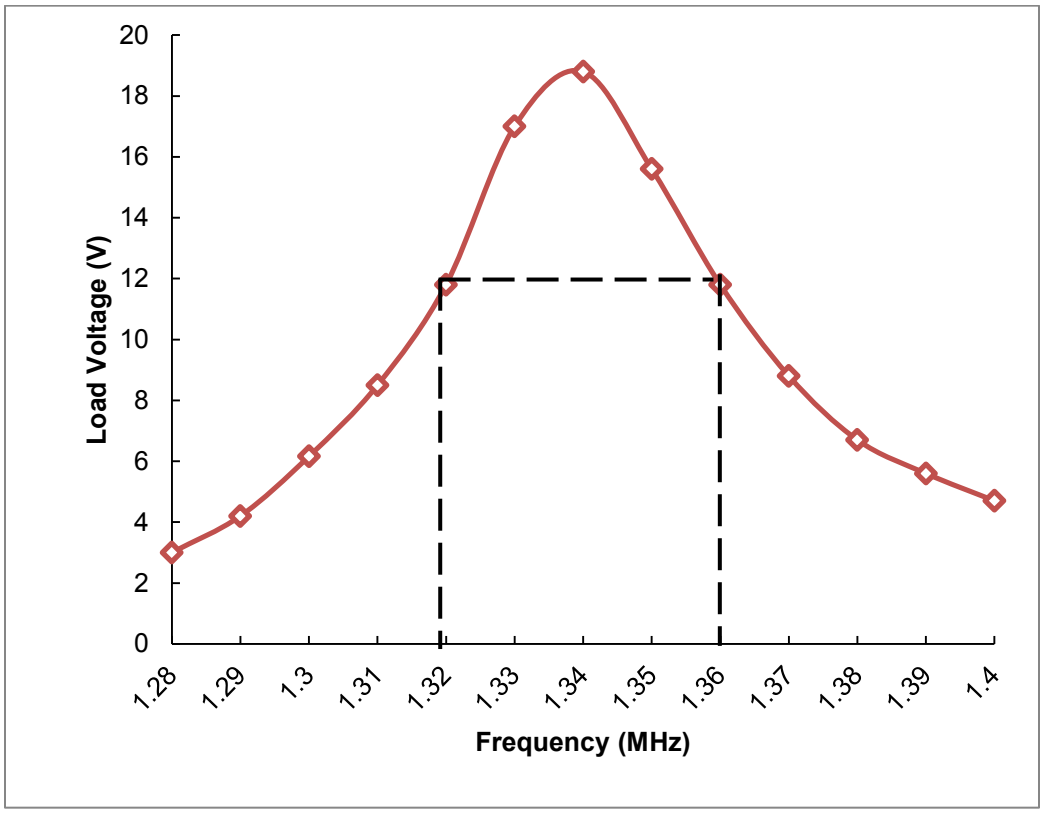

Figure 4.14 Transmitter frequency vs. output voltage across 500 Ohm load at the receiver

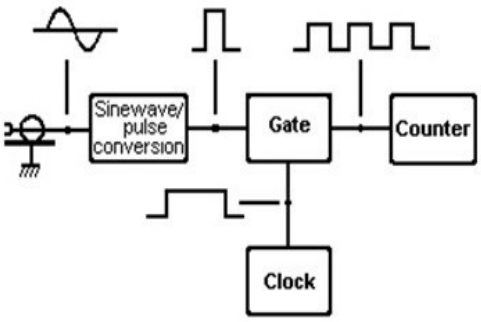

Frequency range	Precise "gate" delay	Resolution
50 MHz - 10 MHz	1 ms	±10 kHz
10 MHz – 1 MHz	5 ms	±2 kHz
1 MHz - 100 KHz	50 ms	±200 Hz
100 Hz - 10 KHz	200 ms	±50 Hz
5 Hz - 50 Hz	310 ms	±2 Hz

Figure 4.15 Frequency counter operation using the controller and Resolution of the counter module for different frequency ranges

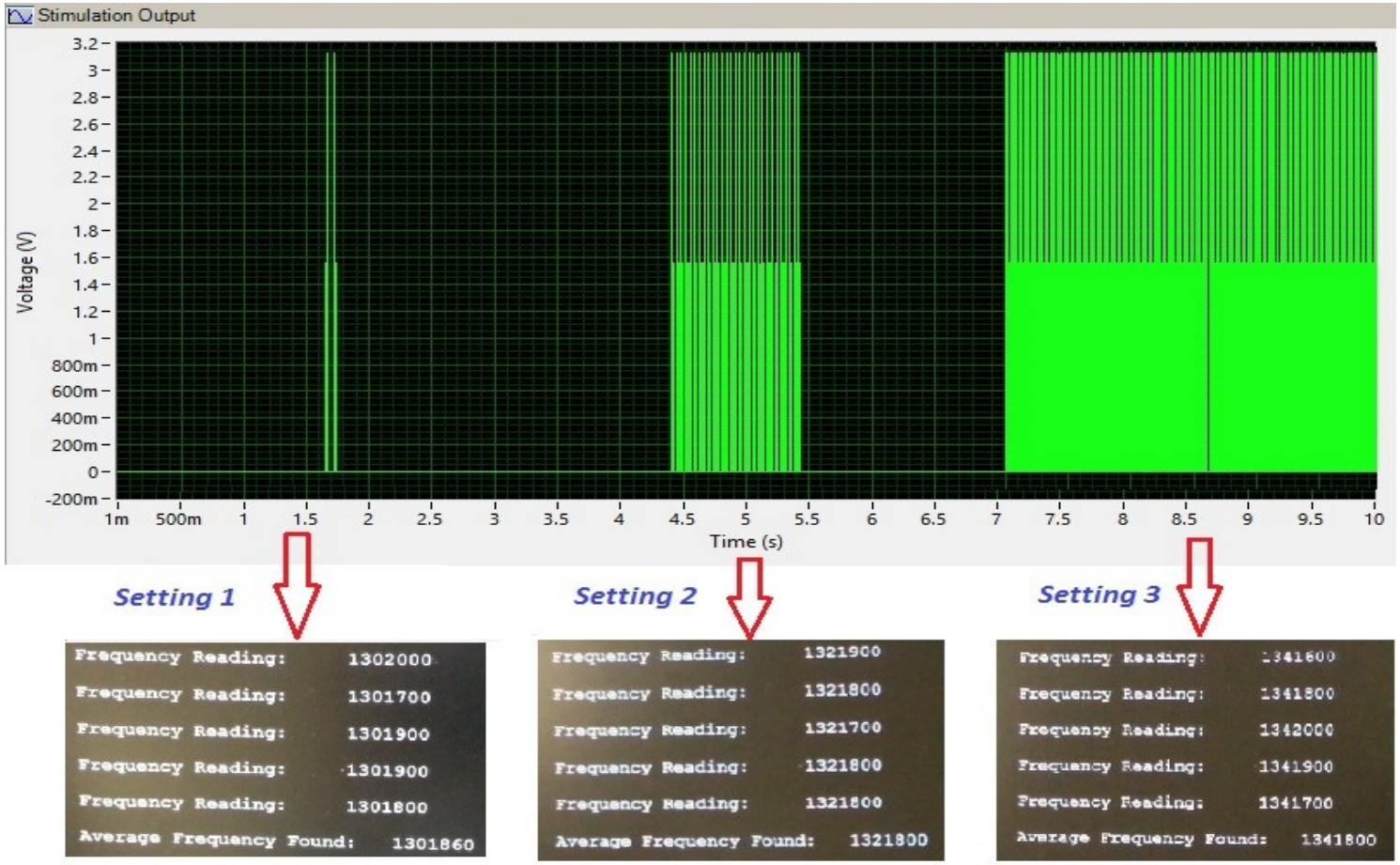

Figure 4.16 Reconfiguration of pulse settings by changing the transmitted frequency

In order to represent the change of setting with the change in transmitted frequency, the average value of the counted frequency is captured in the monitor using RS-232 interface. The stimulation data acquired using DAQ card and LabVIEW is shown along with the average value of the counted frequency in figure 4.14. In this experiment, 1.30 MHz corresponds to low setting; 1.32 MHz is to medium setting and 1.34 MHz changes to high setting.

4.4 Summary

After integrating the PCB board with receiver coil, the overall dimension of the stimulator was 13x7x5 mm^3. When compared to the existing Enterra stimulator this is almost $1/10^{th}$ of size reduction. To give an absolute size comparison, the following figure 4.15 gives a size comparison between iBLISS (Integrated Battery Less Implantable Stimulation System) and existing device Enterra Therapy.

(a)

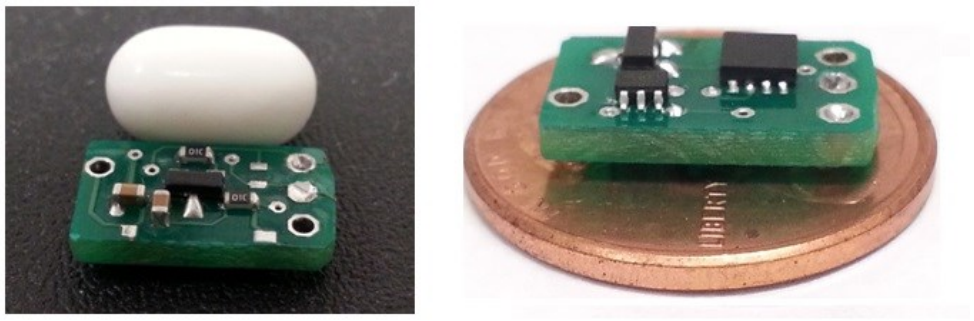

(b)

4.17 (a) Existing configuration Enterra therapy compared half the size of Altoids breathe mint box (b) iBLISS compared to the size of penny

CHAPTER 5

CONCLUSION AND FUTURE WORKS

5.1 Conclusion

In this work, miniaturized and wireless gastrostimulator is demonstrated. The size was reduced by 50% compared to the previous research work carried out on this application. It can be more easily implanted through endoscopic method. Also, it can be implanted through minimal invasive surgery, since the overall device size is very small compared to existing configuration. The wireless power transfer for the miniaturized device was demonstrated up to 10cm. Also, in this work different transmitter and receiver configurations were analyzed and their efficiency was investigated. A comprehensive optimization procedure was carried out while designing this prototype so that maximum power can be transferred from the transmitter to the implant. The threshold current of 5 mA was obtained even at the distance of 10 cm. The device is small enough to be implemented in freely moving animals. Hence, the research work can be extended to carry out hassle free animal experiments. Finally, a new innovative method to reconfigure the stimulator settings without using any wireless communication device has been demonstrated in this work. This is big breakthrough in terms of clinical applications. The patient need not undergo further invasive surgery to change the setting in future. This research work paves a way to efficiently transfer the power for all kinds of implantable devices. The wireless experiments carried out in this work can be extended to other implantable medical applications.

5.2 Future Works

5.2.1 Wearable Transmitter Module

The idea of this section is to come up with the wearable transmitter module. The proposed design is to have the entire transmitter module on a wearable jacket or a specially designed light weigh belt.

The transmitter module is currently tested at bench top experiment. The proposed design will be fabricated on a planar PCB. The transmitter antenna made with AWG-24 wire and 17 turns will be used in this design. The class-E amplifier design was optimized and operated in saturation region in order to increase the battery endurance. The function generator (Agilent Model) will be replaced by a pre-programmed rfPIC controller module. This microcontroller will be pre-programmed to generate 1.3 MHz carrier signal by using DDS technique. Lithium-ion batteries will be used for powering up the class-E amplifier and controller. By using low drop out regulator the controller will be powered using the same battery source. The block diagram of the proposed wearable transmitter module is shown in figure 5.1.

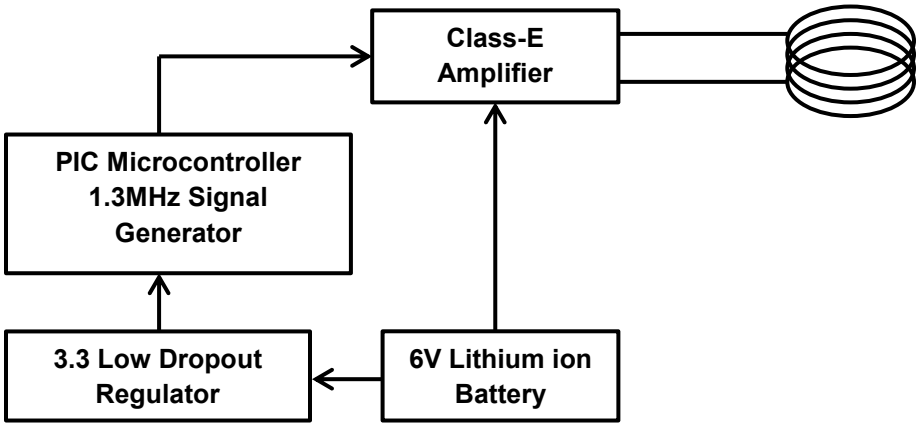

Figure 5.1 Wearable transmitter module

5.2.2 Flexible Implant Module

The flexible printed circuit board is gaining greater significance in modern hardware design. With flexible board, the stimulator can be implanted through the mucosa region with

very small invasive surgery. Hence, it is proposed to extend the design of miniaturized stimulator given above in to a flexible PCB. The substrate used will be flexible polyamide materials such as kapton. As the initial step nickel and gold are metal deposited using e-beam deposition technique. The fabrication steps will involve metal deposition, followed by photolithography and wet etching for creating the required patterns. The SMD soldering will be performed consecutively and the prototype will go through feasibility and reliability tests.

5.2.3 Tissue Effects

In order to study the attenuation effects based on the human tissue and its impact on wireless power transfer, series of experiments will be conducted my mimicking the tissue material. The wireless experiments will be carried out with NaCl (Sodium Chloride) solution and with the pork meat as the medium between transmitter and stimulator. These experiments will help us estimate the resonance shifts due to parasitic involved in this. Also, it will help to predict the efficiency of the device accurately in the presence of tissues. The reason being human body consists of plenty of salts; hence by replicating these tests will lead us to predict the actual system behavior. The concentration of NaCl solution can be varied and the plot of attenuation with distance can be obtained. Figure 5.2 represents the test bench setup for carrying out attenuation tests by using NaCl solution.

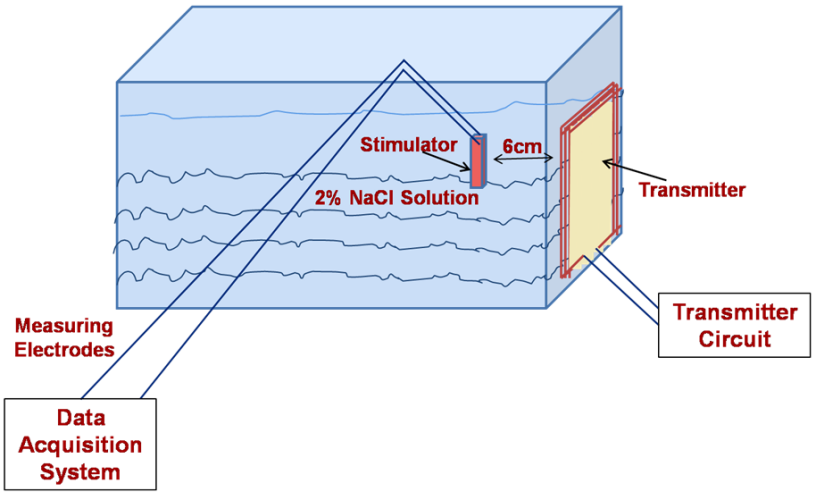

Figure 5.2 Proposed test setup for predicting attenuation with NaCl solution

Appendix A

PROGRAM IN C LANGUAGE FOR THE GASTROSTIMULATOR MODULE WITH RECONFIGURATION FEATURE

```
#include <htc.h>
volatile int count=0;
#include <string.h>
#include <stdlib.h>
#include <stdio.h>

#define _XTAL_FREQ 1000000 //4MHz

void init(void)
{

   TRISA   = 0b00100000;
   LATA    = 0b00000000;
   TXCKSEL = 0b1;            // TX Function is on RA4

   CCP1SEL                 = 0b0;        // CCP1 is on RA2 (Pin 5)
   CCP1CON     = 0b00011100;
   CCPR1L      = 0b00000001;

   T2CON       = 0b00000111;

   //OPTION_REG  = 0b00000000;
   //TMR0        = 194;
   //TMR0IE      = 1;
}


void init_usart(void)
{
  SPBRG = 12;               // Baud Rate : 19200 @ 1MHz
  BRG16 = 1;
  TXSTA = 0b00100100;        // 8 bits, TX on, Async, High Speed
  RCSTA = 0b10000000;        // Serial Port On, 8bit,
}

void Serial_PutC(char str)
{
 while(!TXIF);
  TXREG=str;
}

void Serial_PutUnsigned(long int x)
{
          char temp;
          unsigned trunc;
          unsigned r;

          trunc = x / 1000000;
          Serial_PutC(trunc + 48);
          x -= trunc*1000000;

          trunc = x / 100000;
```

```
            Serial_PutC(trunc + 48);
            x -= trunc*100000;

            trunc = x / 10000;
            Serial_PutC(trunc + 48);
            x -= trunc*10000;

            trunc = x / 1000;
            Serial_PutC(trunc + 48);
            x -= trunc*1000;

            trunc = x / 100;
            Serial_PutC(trunc + 48);
            x -= trunc*100;

            trunc = x / 10;
            Serial_PutC(trunc + 48);
            x -= trunc*10;

            trunc = x;
            Serial_PutC(trunc + 48);
}


void Serial_PutS(char sStr[])
{
  int iCount,iStrlen;
  iStrlen=strlen(sStr);
  for(iCount=0;iCount<iStrlen;iCount++)
     Serial_PutC(sStr[iCount]);
 }

void frequency()
{   long int frequency[5], freq=0, dummy=0;
    int i=0;
    char sStr[10];
      __delay_ms(5000);
     for(i=0;i<5;i++)
      {
       T1CON = 0b10000101;   // Enable Timer 1
       __delay_ms(10);
       T1CON = 0b10000100;   // Disable Timer 1
                    frequency[i] = TMR1;
       frequency[i] = frequency[i] *100;
       dummy=frequency[i];
       freq+=frequency[i];
                    TMR1 = 0;

       __delay_ms(100);
       Serial_PutS("\r\n\t\tFrequency Reading:     ");
       __delay_ms(100);
                    Serial_PutUnsigned(dummy);
```

```
        __delay_ms(100);
        Serial_PutS("\r\n");
       }

        freq=freq/5;

        __delay_ms(10);
        Serial_PutS("\r\n\t\tAverage Frequency Found:   ");
        __delay_ms(10);
                    Serial_PutUnsigned(freq);
        __delay_ms(10);
        Serial_PutS("\r\n");
        __delay_ms(10);

        //OSCCON= 0b11011011;     // 1 MHz Internal Oscillator
        if(freq<=1315555)
            { PR2 = 72;
              __delay_ms(100);
              Serial_PutS("\r\n\t\tThats Setting 1 !!!\r\n ");
            }
        else if(freq>1315555 && freq<1335555)
             { PR2 = 140;
               __delay_ms(100);
               Serial_PutS("\r\n\t\tThats Setting 2 !!!\r\n");
            }
        else if(freq>=1335555)
            { PR2 = 255;
              __delay_ms(100);
              Serial_PutS("\r\n\t\tThats Setting 3 !!! \r\n");
            }
}

void main(void)
{
            init();
    init_usart();
    OSCCON      = 0b11011011;    // 1 MHz Internal Oscillator

        __delay_ms(100);
        Serial_PutS("\r\n\t\tWelcome to Gastrostimulator Project..!");
        __delay_ms(100);
        Serial_PutS("\r\n\t\t(c) Guru Moorthy Ravi 2012-13, iMEMS group");
        __delay_ms(100);
        Serial_PutS("\r\n");


    while(1)
    {frequency();
    }

}
```

```
while(1)
   {
      if(TMR0IE == 1 && TMR0IF == 1)
        {  count++;
           if(count == 2500)
            {  T2CON = 0b00000011;
            }
           else if(count == 2500)
            {  T2CON = 0b00000111;
               count = 0;
            }
           TMR0IF=0;
        }
   }
```

REFERENCES

[1] IEEE standard for safety levels with respect to human exposure to radio frequency electromagnetic fields, 3 kHz to 300 GHz. *IEEE Std C95. 1-2005 (Revision of IEEE Std C95. 1-1991)* pp. 0_1-238. 2006.

[2] J. A. Doherty, G. A. Jullien and M. P. Mintchev. Transcutaneous powering of implantable micro-stimulators for functional restoration of impaired gastrointestinal motility. Presented at Engineering in Medicine and Biology Society, 2003. Proceedings of the 25th Annual International Conference of the IEEE. 2003, .

[3] J. A. Doherty, G. A. Jullien and M. P. Mintchev. Transcutaneous powering of implantable micro-stimulators for functional restoration of impaired gastrointestinal motility. Presented at Engineering in Medicine and Biology Society, 2003. Proceedings of the 25th Annual International Conference of the IEEE. 2003, .

[4] P. Scholz, C. Reinhold, W. John and U. Hilleringmann. Analysis of energy transmission for inductive coupled RFID tags. Presented at RFID, 2007. IEEE International Conference on. 2007, .

[5] P. Scholz, C. Reinhold, W. John and U. Hilleringmann. Analysis of energy transmission for inductive coupled RFID tags. Presented at RFID, 2007. IEEE International Conference on. 2007, .

[6] P. R. Troyk and G. A. DeMichele. Inductively-coupled power and data link for neural prostheses using a class-E oscillator and FSK modulation. Presented at Engineering in Medicine and Biology Society, 2003. Proceedings of the 25th Annual International Conference of the IEEE. 2003, .

[7] Yong-Hae Kim, S. Kang, Myung-Lae Lee, Byung-Gon Yu and T. Zyung. Optimization of wireless power transmission through resonant coupling. Presented at Compatibility and Power Electronics, 2009. CPE '09. 2009, .

[8] Yong-Xin Guo, Duan Zhu and R. Jegadeesan. Inductive wireless power transmission for implantable devices. Presented at Antenna Technology (iWAT), 2011 International Workshop on. 2011, .

[9] T. Abell, R. McCallum, M. Hocking, K. Koch, H. Abrahamsson, I. Leblanc, G. Lindberg, J. Konturek, T. Nowak, E. M. Quigley, G. Tougas and W. Starkebaum. Gastric electrical stimulation for medically refractory gastroparesis *Gastroenterology 125(2),* pp. 421-428. 2003.

[10] T. Abell, R. McCallum, M. Hocking, K. Koch, H. Abrahamsson, I. Leblanc, G. Lindberg, J. Konturek, T. Nowak, E. M. Quigley, G. Tougas and W. Starkebaum. Gastric electrical stimulation for medically refractory gastroparesis *Gastroenterology 125(2),* pp. 421-428. 2003.

[11] C. F. Andren, M. A. Fadali, V. L. Gott and S. R. Topaz. The skin tunnel transformer. A new system that permits both high efficiency transfer of power and telemetry of data through the intact skin *IEEE Trans. Biomed. Eng. 15(4),* pp. 278-280. 1968.

[12] P. M. Boyce, N. J. Talley, C. Burke and N. A. Koloski. Epidemiology of the functional gastrointestinal disorders diagnosed according to rome II criteria: An australian population-based study *Intern. Med. J. 36(1),* pp. 28-36. 2006.

[13] A. D. DeHennis and K. D. Wise. A wireless microsystem for the remote sensing of pressure, temperature, and relative humidity *J Microelectromech Syst 14(1),* pp. 12 <last_page> 22. 2005.

[14] J. C. Eagon and K. A. Kelly. Effect of electrical stimulation on gastric electrical activity, motility and emptying *Neurogastroenterol. Motil. 7(1),* pp. 39-45. 1995.

[15] J. C. Eagon and K. A. Kelly. Effect of electrical stimulation on gastric electrical activity, motility and emptying *Neurogastroenterol. Motil. 7(1),* pp. 39-45. 1995.

[16] S. Islam, L. R. Vick, M. J. Runnels, J. R. Gosche and T. Abell. Gastric electrical stimulation for children with intractable nausea and gastroparesis *J. Pediatr. Surg. 43(3),* pp. 437-442. 2008.

[17] M. P. Jones, C. C. Ebert and K. Murayama. Enterra for gastroparesis *Am. J. Gastroenterol. 98(11),* pp. 2578. 2003.

[18] Z. Lin, J. Forster, I. Sarosiek and R. W. McCallum. Treatment of gastroparesis with electrical stimulation *Dig. Dis. Sci. 48(5),* pp. 837-848. 2003.

[19] C. Moldovan, D. L. Dumitrascu, L. Demian, C. Brisc, L. Vatca and S. Magheru. Gastroparesis in diabetes mellitus: An ultrasonographic study *Rom. J. Gastroenterol. 14(1),* pp. 19-22. 2005.

[20] Qianhong Chen, Siu Chung Wong, C. K. Tse and Xinbo Ruan. Analysis, design, and control of a transcutaneous power regulator for artificial hearts *IEEE Transactions on Biomedical Circuits and Systems 3(1),* pp. 23-31. 2009.

[21] C. Reinhold, P. Scholz, W. John and U. Hilleringmann. Efficient antenna design of inductive coupled RFID-systems with high power demand *Journal of Communications 2(6),* 2007.

[22] M. L. S Haddab. Microcontroller-based system for electrogastrography monitoring through wireless transmission *Measurement Science Review 9*2009.

[23] K. M. Silay, C. Dehollain and M. Declercq. 2008 ph.D. research in microelectronics and electronics; improvement of power efficiency of inductive links for implantable devices 2008, .

[24] I. Soykan, B. Sivri, I. Sarosiek, B. Kiernan and R. W. McCallum. Demography, clinical characteristics, psychological and abuse profiles, treatment, and long-term follow-up of patients with gastroparesis *Dig. Dis. Sci. 43(11),* pp. 2398-2404. 1998.

[25] P. R. Troyk and M. A. Schwan. Closed-loop class E transcutaneous power and data link for microimplants *IEEE Trans. Biomed. Eng. 39(6),* pp. 589-599. 1992.

[26] K. D. Wise, D. J. Anderson, J. F. Hetke, D. R. Kipke and K. Najafi. Wireless implantable microsystems: High-density electronic interfaces to the nervous system *Proc IEEE 92(1),* pp. 76 <last_page> 97. 2004.

[27] J. Xu, R. A. Ross, R. W. McCallum and J. D. Chen. Two-channel gastric pacing with a novel implantable gastric pacemaker accelerates glucagon-induced delayed gastric emptying in dogs *Am. J. Surg. 195(1),* pp. 122-129. 2008.

[28] Young-Sik Seo, Minh Quoc Nguyen, Z. Hughes, S. Rao and J. -. Chiao. 2012 IEEE/MTT-S international microwave symposium digest; wireless power transfer by inductive coupling for implantable batteryless stimulators 2012, .

BIOGRAPHICAL INFORMATION

Guru Moorthy Ravi received his Bachelor's Degree in Electronics and Communication Engineering from Anna University, Chennai, India in the year 2010. He is university rank holder and distinguished student of Electrical Engineering Department. He worked as Project Graduate Assistant at Avionics Division, National Aerospace Laboratories (NAL) at Bangalore, India during 2010-11. His major contributions at NAL are Autopilot Hardware Design for Micro Air Vehicles, System and Timing Analysis for Integrated Modular Avionics (IMA). He received Council for Scientific and Industrial Research (CSIR) Student Scholarship for the year 2010-11 from Government of India. He joined as Master's Student at University of Texas Arlington (UTA) in the year 2011. He also did his Internship at CUDD Energy Services at Odessa, Texas providing Electrical Engineering Technical Support in May 2012. He received UTA Optics Scholarship award for the academic year 2011-12. His areas of interests are Circuit Design, Wireless Power Transfer, Embedded Systems Design, Board & Card level Hardware Design and MEMS. He received his Master's Degree in Electrical Engineering in spring 2013. He is active member of Electrical Engineering Honor Society Eta Kappa Nu (HKN), Epsilon Mu Chapter and IEEE Fort Worth Chapter. He also served as International Peer Advisor (IPA) at Office of International Education (OIE), UTA during spring 2013. He is volunteer and member at UT Arlington Leadership Academy. His hobbies are Judo, Hiking, Music and Star Gazing.